



Assignment of master's thesis

Title: Evacuation model with leading and following agents focused on evacuation of (pre)schools

Student: Bc. Matej Šutý

Supervisor: Ing. Pavel Hrabák, Ph.D.

Study program: Informatics

Branch / specialization: Knowledge Engineering

Department: Department of Applied Mathematics

Validity: until the end of summer semester 2023/2024

Instructions

The thesis should combine the idea of using a hierarchical system of multi-agent coordination for evacuation simulations (developed in Janovská, 2021) with expert knowledge on pre-school children's behaviour during evacuation (captured by Najmanová, 2020). The work should result in an evacuation model/software prototype, where the dynamics of the following agents (children) are consistent with the expert knowledge, and the planning actions of leading agents (teachers) are inspired by real-world instructions and limitations.

1. Survey evacuation models enabling assisted evacuation with a focus on evacuation of (pre)-school activities. Focus on cellular models.
2. Survey studies dealing with applications of multiagent planning algorithms in evacuation simulations.
3. In cooperation with the fire engineering expert (H. Najmanová) identify basic principles of children's behaviour and teachers' activities during evacuation. Suggest a transformation of those principles to rules of agent interaction in the cellular model.
4. Design and implement the cellular model of evacuation with the above-mentioned features enabling the application of planning algorithms for the actions of leading agents.
5. Perform several simulation experiments and compare various leading agent strategies with respect to total evacuation time.



**FACULTY
OF INFORMATION
TECHNOLOGY
CTU IN PRAGUE**

Master's thesis

Evacuation model with leading and following agents focused on evacuation of (pre)schools

Bc. Matej Šutý

Department of Applied Mathematics
Supervisor: Ing. Pavel Hrabák, Ph.D.

May 4, 2023

Acknowledgements

In the first place, *it is truly right and just* to give thanks to God for being with Him during this research. I am very grateful for everyone in my family - you help me constantly and care for me beyond what I deserve. This research would not be possible without the help of Pavel Hrabák, who went over and beyond to guide me in the fascinating world of academic research, and I am deeply grateful for it.

Declaration

I hereby declare that the presented thesis is my own work and that I have cited all sources of information in accordance with the Guideline for adhering to ethical principles when elaborating an academic final thesis.

I acknowledge that my thesis is subject to the rights and obligations stipulated by the Act No. 121/2000 Coll., the Copyright Act, as amended, in particular that the Czech Technical University in Prague has the right to conclude a license agreement on the utilization of this thesis as a school work under the provisions of Article 60 (1) of the Act.

In Prague on May 4, 2023

.....

Czech Technical University in Prague
Faculty of Information Technology
© 2023 Matej Šutý. All rights reserved.

This thesis is school work as defined by Copyright Act of the Czech Republic. It has been submitted at Czech Technical University in Prague, Faculty of Information Technology. The thesis is protected by the Copyright Act and its usage without author's permission is prohibited (with exceptions defined by the Copyright Act).

Citation of this thesis

Šutý, Matej. *Evacuation model with leading and following agents focused on evacuation of (pre)schools*. Master's thesis. Czech Technical University in Prague, Faculty of Information Technology, 2023.

Abstrakt

Děti, které tvoří významnou část populace, jsou spolu s nemocnými, staršími a zdravotně postiženými nejzranitelnější skupinou během evakuace. Nové výzkumní experimenty na chování a pohyb dětí během evakuace v mateřských školách v České republice nabízejí pevnou teoretickou základnu pro vývoj simulačního modelu, který zachycuje specifické chování dětí.

Navržený model v této práci je hierarchický systém vedoucích a následujících agentů koordinovaných pomocí centrálního plánovacího algoritmu. Je založen na extended floor field modelu. Hlavní přínos spočívá v analýze nových strategií a pravidel pro vedoucího agenta, jako je pozice ve skupině. Struktura skupiny je zachycena zavedením tvorby dvojic dětí pohybujících se ve frontách a vlivu vedoucího agenta na následující agenty. V závěru práce jsou diskutována omezení a nabízí se výhled možných zlepšení.

Klíčová slova Hierarchický model, simulace evakuace dětí, vedoucí a následující agenti, agentní model, tvorba dvojic, extended floor field model, celulární automat

Abstract

Children, who account for a significant part of the population, are among the most vulnerable during evacuation, along with the sick, elderly, and disabled. Recent experimental research conducted in preschools in the Czech Republic has provided a theoretical foundation for developing a simulation model that captures children's specific behavior during evacuation.

The model proposed in this thesis is a hierarchical system of leading and following agents coordinated by a central planning algorithm. It is based on an extended floor field model. The main contribution of this work lies in analyzing novel strategies and rules for the leading agent, such as its position within the crowd. The crowd structure is modeled by introducing a pair formation of children moving in queues and examining the leader's

influence over the following agents. Finally, the thesis discusses limitations and suggests possible areas for future improvement.

Keywords Hierarchical model, simulation of children evacuation, leading and following agents, agent based model, pair formation, extended floor field model, cellular automaton

Contents

Introduction	1
1 Theoretical background and literature review	3
1.1 Research of guided movement and evacuation of children	3
1.2 State-of-the-art models	5
1.3 Planning	8
1.4 Theoretical baseline	9
2 Analysis and design	11
2.1 Hierarchical model	11
2.2 Methods	12
2.3 Strategies and rules	19
3 Implementation	27
3.1 Mesa	30
4 Simulation experiments	33
4.1 Maps	33
5 Results	37
5.1 Gaps between pairs	37
5.2 Pair formation	38
5.3 Symmetry of the experiments	40
5.4 Total evacuation time	40
5.5 Penalization parameter	43
5.6 Specific flow	44
5.7 Sensitivity to static field parameter	46
5.8 Sensitivity to occupied cell parameter	48
5.9 Limitations	49
Conclusion	51
Bibliography	53
A Acronyms	57
B Further graphical output	59
C Contents of enclosed CD	63

List of Figures

1.1	Photo from experimental evacuation of children from train. Image taken from [1].	4
1.2	Typical pedestrian group formations while walking. Image taken from [2].	4
1.3	Example of leader-follower structure in UAV coordination model. Image taken from [3].	5
1.5	Agent based model of macroscale city evacuation where population characteristics are assigned to individual agents. Image taken from [4].	6
1.4	Moore neighbourhood of an agent and 9 possible movements.	6
1.6	Potential field which describes the distances from multiple exits used in CA model. Image taken from [5].	7
1.7	CA model with smart planning module adapts to pedestrian distribution acquired from IoT monitoring. Image taken from [6].	8
2.1	Map <code>small.txt</code> initialized.	11
2.2	Directed agent is oriented to North. Arrows show resulting orientation after moving to cells in Moore neighbourhood.	14
2.3	Example of pair formation in few steps of simulation. Initial positions of directed agents are on the left. The middle figure shows first paired agents. The right figure shows all agents formed in pairs apart from the isolated agents.	15
2.4	Simple maneuvers of paired agents that do not change leadership. Leader in the pair is painted black.	16
2.5	Complex maneuvers of paired agents that change leadership. Leader in the pair is painted black.	17
2.6	Virtual leading agent (white circle) sets SFF with its location as goal. Leading agent (black circle) is positioned at back of the crowd.	18
2.7	Visualization of specific children behavior during evacuation. Image taken from [7].	19
2.8	Leader strategy standing guard at a location and waiting (left), following agents passing the leader and navigating towards goal (right).	20
2.9	Penalization decreases with distance to the leader.	21
2.10	Two situations where a different correct orientation is selected based on the position of the leader, which is colored black with smaller white circle inside. On the left, the maneuvers for paired agents directed to North which result in North orientations are not penalized. On the right, the leader passed the corner and the paired agents should turn to South. Maneuvers resulting in other orientation than South are penalized.	22
2.11	Simulations with penalization value 1 in the top figure show few incorrect maneuvers compared to bottom figure where penalization is 0.	23

2.12	Agent crosses an obstacle. This movement is penalized, although possible.	24
2.13	With exit placed at the South, the simple maneuvers on the left are not penalized. The diagonal maneuver in the top right results in correct orientation but the white agent is passing an obstacle thus obstacle penalization is applied. The complex maneuver in the bottom right is not penalized but black agent τ is increased with twice the movement duration.	24
2.14	Leader position at the back (left) and at the front of the crowd (right).	25
3.1	Schema of one simulation run.	27
3.2	Task flow in one step of <i>SequentialActivation</i> object.	28
3.3	Three agents form a cycle, which is detected and broken. The arrows indicate their desired cell in the next move.	29
3.4	Visualization of evacuation simulation in browser.	32
4.1	Initial positions and goals of leading and following agents in the classroom <code>mapX1.txt</code>	33
4.2	Initial positions and goals of leading and following agents in the classroom <code>mapX2.txt</code>	33
4.3	Initial positions and goals of leading and following agents in the classroom <code>mapX3.txt</code>	35
4.4	Illustration of maps <code>gaps.txt</code> on the top and <code>gaps_back.txt</code> on the bottom. Trigger points are depicted as yellow cells and dots show the cells that were hidden due to the length of the map.	35
5.1	Distance between individual pairs in map <code>gaps.txt</code> and <code>gaps_back.txt</code> is consistent. Each histogram shows a distance of a pair to pair in front of them. The y axis shows counts of the distances in the investigated area across all simulations.	38
5.2	Distance of agents to the leader of <code>map01.txt</code> in the top figure, <code>map02.txt</code> in the middle figure, <code>map03.txt</code> in the bottom figure.	39
5.3	Distance of agents to the leader of <code>map21.txt</code> in the top figure, <code>map22.txt</code> in the middle figure, <code>map23.txt</code> in the bottom figure.	41
5.4	Distribution of distances of agents to the leading agent in <code>map21.txt</code>	42
5.5	Heatmap of cell visits shows symmetry in <code>map23.txt</code> on top and the mirrored version below it.	42
5.6	Boxplot of distances to the leading agent in original map <code>map23.txt</code> and mirrored map <code>map23.txt</code>	43
5.7	Penalization 0 in top figure, 0.5 in middle and 1 at the bottom. Ratio of maneuvers resulting in incorrect orientation decreases with higher penalization.	44
5.8	From left to right, top to bottom, specific flow for <code>map01.txt</code> , <code>map02.txt</code> , <code>map03.txt</code>	45
5.9	From left to right, top to bottom, specific flow for <code>map21.txt</code> , <code>map22.txt</code> , <code>map23.txt</code>	46
5.10	Heatmap of visits of cells in <code>map23.txt</code> with $k_S = 1$ in graph on the top, $k_S = 3$ in the middle, $k_S = 5$ on the bottom.	47
5.11	k_O with values of 0 on the top, 0.5 in the middle and 1 on the bottom in <code>map22.txt</code>	48
B.1	Simulations with <i>Baseline</i> parameters in <code>map23.txt</code> on the left and in <code>map23_mirror.txt</code> on the right show comparable distribution of TET.	59
B.2	From the left top to right bottom, specific flow for <code>map11.txt</code> , <code>map12.txt</code> , <code>map13.txt</code>	60

List of Tables

4.1	Goals of each map	34
4.2	Parameter values for simulation experiments	36
5.1	Comparison of path lengths for different scenarios	43

Introduction

Evacuation is a critical aspect of ensuring safety in crowded public spaces, such as schools, offices, and commercial buildings. The behavior of pedestrians during evacuation is complex and can be influenced by a range of factors, such as the size of the space, the number of people, and the presence of obstacles. Furthermore, the behavior of children during evacuation differs from that of adults, and the movement abilities of children are highly age-dependent. Children account for a big portion of population and together with elderly, sick or disabled people are the most vulnerable group which requires more attention during evacuation. In recent years, there has been an increased focus on the study of pedestrian behavior during evacuation, especially in the context of high-density conditions and group dynamics. However experimental simulations which model the specific movement of children are missing.

This thesis aims to provide insights into the behavior of pedestrians during evacuation and proposes a novel approach to evacuation simulation, particularly in the context of preschool children. The proposed research addresses a gap in the literature by analyzing the organized evacuation of children using a hierarchical model where the leading agent is responsible for the navigation of following agents to the current goal. The hierarchical model makes use of various strategies and rules that define the movement of leading and following agents and together with a planning module allows for simulation of wide range of situations. The prototype model was developed in consultation with fire engineering expert to follow the specific dynamics of preschool children and real world instructions and limitations.

By exploring the importance of guidance and group dynamics in pedestrian crowd evacuation, we aim to contribute to the development of more effective evacuation strategies and improve the safety of crowded public spaces.

Theoretical background and literature review

The simulation of evacuation dynamics is already a well-established and frequently researched topic throughout the world. Only recently, the world population rose to 8 billion people, and more and more people moved to densely populated cities. The change in the urban characteristics and the development of new buildings is evident as the demands for safety, effectiveness and comfort increase beyond the state legislation requirements. The ability to "see around the corner" and tackle problems before they appear is vital to agile and intelligent construction of buildings, urban planning and preparation for dangerous events.

Simulation models offer the means to assess complex structures, ranging from single rooms to the scale of whole cities, and capture the dynamics of pedestrian movement of large crowds. The development of such models encounters numerous obstacles, many of which hugely depend on understanding human movement's psychological and physical characteristics. Experimental research is essential in this field and lays the foundations for precise and reliable models. The progress in pedestrian simulation models goes hand in hand with the increased focus on data collection and evaluation of pedestrian movement in workplaces, schools, transition areas and events among others.

Gathering data of the less represented groups is essential, even though it can be challenging. The data, tests and norms for the movement of children, elderly, sick or disabled are scarce and have considerable variance, even though this group represents a significant part of the population which requires more attention.

1.1 Research of guided movement and evacuation of children

The first step in modeling a phenomenon is to observe it and attempt to extract the essential characteristics. Currently the main source of results come from arranged experiments with either informed [7], [1] or uninformed [8] participants, video analysis of various events [9] and also governmental institutions [10]. An example photo from experimental evacuation of children from a double deck train can be seen in Figure 1.1.

The characteristics can be arbitrarily separated to either a) quantitative findings, which capture the objective nature and describe it using numbers, diagrams, graphs and relations, and b) qualitative findings, which allow the insight to the inner nature of evacuation situations and interpret it in a way which can't be pinned down numerically.

Some of earliest data sources of movement of people in public buildings come from 1969, where the person density was introduced and explained. Also flow of different mixture of



Figure 1.1: Photo from experimental evacuation of children from train. Image taken from [1].

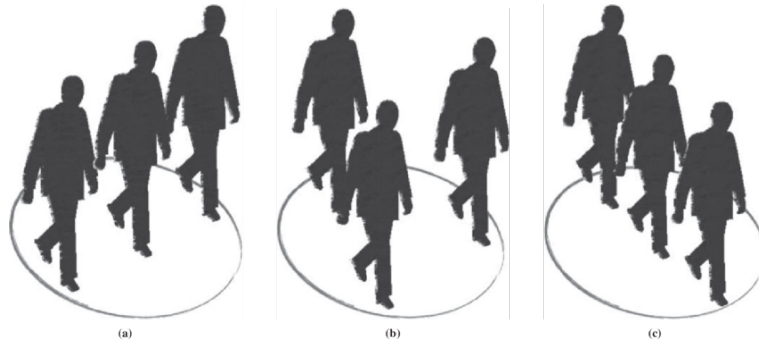


Figure 1.2: Typical pedestrian group formations while walking. Image taken from [2].

people, as used in this thesis, was described in the same research [11]. Nowadays, more complex and precise experimental data emerge. The average speed of groups of different size is thoroughly analyzed in [2]. The authors define typical walking formations of dyads, triads and groups of four such as line abreast, V-like, and riverlike (queue) which are depicted in Figure 1.2. Another finding is the t-test supported significant difference in average path length and speed of single pedestrians compared to pedestrian groups, e.g. the average walking speed of group is 37.21% slower than single pedestrian. The speed constants and formation of walking groups were used as a reference in this thesis.

An empirical study of child evacuation under non-emergency and emergency situations in China revealed qualitative findings in the capabilities of children. The study highlighted the limited cognitive and psychological and physical capabilities, which can result in unpredictable decision making [12]. The results of the study support the claims of age-dependent characteristics of movement in [7]. It is important to mention a high variance in the measured speed of walking and running children of different age:

“...78% of the younger children have a walking speed of 0.41m/s to 0.80m/s and more than 66% of the older children have a walking speed in the range of 0.6m/s to 1.00m/s. It is also clear that younger children move slower than the older ones, regardless of whether they are walking or running. The average walking speeds were 0.60m/s and 0.84m/s for the younger and older age group respectively and 1.14m/s for younger and 2.23m/s for older, when the children ran.” [13]

Modeling a system, with such a high variance in the basic structure, is a task which requires extensive testing, validating and constant research.

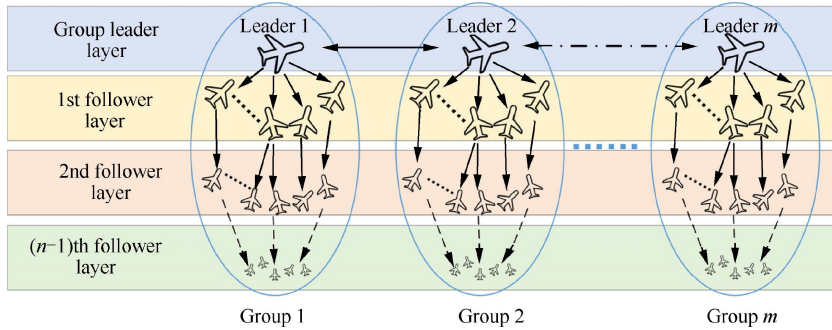


Figure 1.3: Example of leader-follower structure in UAV coordination model. Image taken from [3].

The qualitative contribution to the evacuation of children lies in the analysis of guides. Examination of real world children environments - family houses, preschools, schools, hobbies - shows, that children are heavily influenced by the adult figures (parents, older siblings, teachers, coaches), that guide children in both non-emergency and emergency situations. The effect of a guide or a leader on the evacuation of group resulted in more accurate overall crowd evacuation time in special cases of people with social ties and within limitations described in [14]. Furthermore, leadership is a major factor in decision-making during evacuation [15]. Najmanová confirmed the hypothesis that children react first to the instructions of adults and only then take into consideration the warning signals and concluded:

“...In most cases, children reacted first to instructions given by adults and not on the warning signal as such. Those situations were well illustrated when a staff member required longer time for signal interpretation. Within this interval, children did not act individually on the warning signal but they waited for the adult’s decision what to do.” [7]

Contrary to this, a survey among elementary students on evacuation route choice in classroom showed surprising results:

“Position, congestion, group behavior and backtracking behavior have significant effects on children’s route choice. Gender and guidance have no prominent impacts on children’s route choice. Age only affects children’s backtracking behavior.” [16]

The opposing findings show how little we know so far about the influence of the mentioned phenomena.

1.2 State-of-the-art models

In several decades of pedestrian evacuation research a number of modelling approaches were introduced. The models range from ones developed in academic research to explore specific phenomena up to proprietary commercial solutions for large projects. The list of models could be even bigger, if models from other fields were included - UAV coordination models [3], road traffic models [17] and game engines [18] among others. The space for interdisciplinary cooperation is large. For example, a similar idea to leader-follower structure presented in this thesis can be seen in the Figure 1.3, where UAV drones are coordinated by swarm algorithm.

Because of the large size of current evacuation models landscape this study will concentrate on the cellular models and their application in the preschool environment. The



Figure 1.5: Agent based model of macroscale city evacuation where population characteristics are assigned to individual agents. Image taken from [4].

literature research aligns with the aim to develop a hierarchical system of planned multi-agent coordination for evacuation simulations in the preschool environment.

Cellular automaton models (CA) typically use a discretized grid of cells (rectangular as can be seen in Figure 1.4, hexagonal or other type) and a simple set of rules to update the cell state. The most famous example is the Game of life [19], where each cell can be in one of two states (alive or dead) and updates the state based on the number of alive cells in its neighborhood. Even though the model structure seems simple, the model creates complex patterns and it was found that one could even create a Turing complete machine using the patterns as logical gates [20]. Nowadays, the CA structure is used in evacuation simulation models as a component in agent based modeling (ABM).

ABM represents pedestrians as individual agents based in some environment. The agents can sense the environment (for example the state of cells in the neighborhood, the agents in their proximity), process it using rules, strategies, schemes and react accordingly. Agent based models can capture heterogeneous individuals which react to local environment, for example in their line-of-sight or other type of neighborhood, which is similar to how people operate in real life. At the same time, the agents can be controlled centrally and share information with each other. All these features make for a great framework to simulate pedestrian movement. Agent based models can scale to simulate large cities as can be seen in the Figure 1.5.

A prime example of simulation model of children evacuation is described in [21]. The model is based on extended CA and simulates the movement of small family groups in the hospital. The parents are modeled as leading agents and children as following agents, that can overlap with leading agents. The importance of groups and relationships between agents in the group are analyzed. The results show, that parents and children have specific behavior characterized by moving at different speeds, the ability to cradle small children in arms and also parents waiting for children to rejoin the group in case of splitting. The family groups in the research consisted of 2 to 4 persons, which is very different from the preschool environment, where staff-to-child ratio is higher. The simulations modeled a

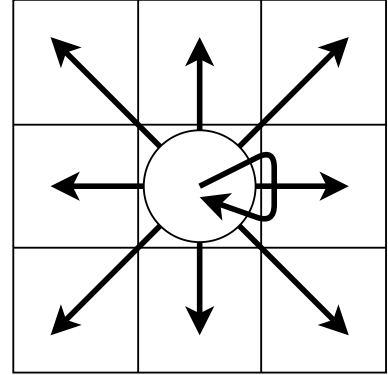


Figure 1.4: Moore neighbourhood of an agent and 9 possible movements.

first floor of pediatric hospital, where the main corridor was more than 100 m long and the main registration area dimensions were $53 \text{ m} \times 35 \text{ m}$. 1500 pedestrians were present at the start of the simulation [21]. The simulated situation can't be compared to the evacuation of a preschool.

Recently, an extended CA model for simulating adult-child matching behavior was presented in China. The study proposed three different strategies for optimizing the evacuation time and modeled the behavior of children using rules. The simulation was situated in a simple room of $2 \text{ m} \times 3.6 \text{ m}$, with cell dimensions $40 \text{ cm} \times 40 \text{ cm}$, where 12 children were matching 12 adults and later evacuating the room together. Interestingly, the exit width was only 40 cm. The simulated situation can be compared to the common event of parents picking up their children from a preschool.

Another current approach integrates the idea of CA models in a hierarchical agent-based model with reinforcement learning. The individual agents, moving on a discrete grid, decide autonomously based on a policy learned with reinforcement learning [22]. The model was validated in benchmark cases (agent moving in corridor, in a turn, etc.) and by comparing the results with particle swarm optimization evacuation model [23]. The study also presented a case study of evacuation of a subway platform. The case study situation does not match the environment examined in this thesis in any aspect. However, the model features a flexible reinforcement learning module, which could potentially capture the specific behavior of children during evacuation.

Another study aimed to understand the children behaviour under non-emergency situations [5]. Missing or limited data of evacuation of children from classroom inspired the research team to conduct a series of experimental evacuations. The analyzed environment was a classroom with dimensions of $7.27 \text{ m} \times 8.74 \text{ m}$, where exit width was 80 cm. There were two exits. In the classroom were 52 students aged between 9 and 11 years and 52 pairs of desks and chairs.

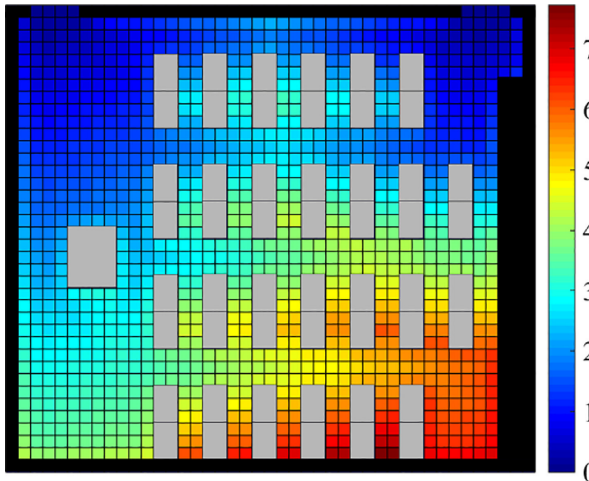


Figure 1.6: Potential field which describes the distances from multiple exits used in CA model. Image taken from [5].

models are representatives of ABM approach, which offers flexible and simple way to model human behavior.

The video footage was analyzed and revealed several patterns of children behavior, which lead to development of CA model to simulate evacuation with these patterns. The classroom was modeled as a grid of 38×43 cells with 52 agents and 52 pairs of desks and chairs. The cell dimensions $20 \text{ cm} \times 20 \text{ cm}$ are different than the most common choice of $40 \text{ cm} \times 40 \text{ cm}$. The choice can be explained that the modeled pedestrians were children, which occupy less space. The visualization of the simulated classroom can be seen in the Figure 1.6.

The foundation for the model in this thesis is a type of CA extended floor field model [24], where the hierarchical structure and planning is inspired by hierarchical swarm model [25]. Both mod-

1.3 Planning

When large number of people with different goals are moving, specific structures and self-organization [26] can be spotted. For example, the movement of people in opposing directions forms a two-lane and a group crossing paths of other groups results in stop and go organization [27]. This way people subconsciously optimize their routes (in terms of length or complexity) and try to minimize the number of conflicts.

The simulation of pedestrian movement which exhibits the desired behavior is challenging. Planning algorithms look at the situations in a bigger picture and cooperate the movements of modeled agents to reconstruct desired phenomena.

Evacuation planning algorithm based on motion and integrated behavior of agents is presented in [28]. The authors construct a roadmap (an abstract path in the configuration space) to the exits for agents in groups. The choice of path in the roadmap minimizes the number of collisions that would slow down the evacuation. This approach is a common practice in robotics planning. The simulation results showed that the evacuation plans were optimized in terms of lower evacuation time. The simulated paths were not compared to evacuation paths from experiments in real world.

Reinforcement learning algorithm was used in [29] to learn and optimize evacuation plan in order to minimize loss of lives. The results show that collaborative agents plan the exploration strategy more effectively than individual agents.

Two strategies of evacuation planning are proposed and simulated in [6], where a digital twin of real life pedestrian is created from internet of things (IoT) monitoring. The digital twin is used to predict movement and adjust the evacuation plan in terms of exit selection. The first strategy is a fixed guidance according to geometry of the building and the second strategy, called smart guidance, estimates evacuation time with simulation using the monitored distribution of agents in the building. It is worth noting, that the authors used CA model for quick repeated simulations. The model overview is depicted in Figure 1.7.

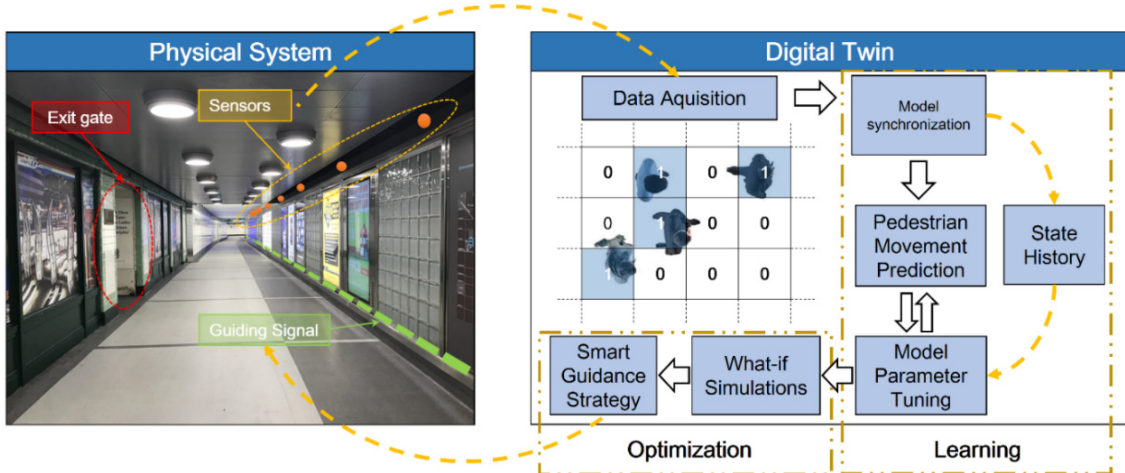


Figure 1.7: CA model with smart planning module adapts to pedestrian distribution acquired from IoT monitoring. Image taken from [6].

The authors in [30] note, that unlike classical planning algorithms, where agents are expected to perfectly obey the central planning authority, the pedestrians in evacuations might deviate from some proposed plan and follow their own. The authors propose a local multi-agent evacuation algorithm (LC-MAE), which relies on local cooperation of agents to make the evacuation paths be more realistic. However, there is an option to have some informed agents which follow the plan. This method aligns with the hierarchical structure

of model proposed in this thesis, where leading agents represent teachers who follow central plan and following agents represent children, who work only with local information and follow the teacher.

In the end, the dimension of planning in current agent based evacuation simulations is present implicitly in the definition of agents' behavior.

1.4 Theoretical baseline

The baseline experimental research on pedestrian evacuation used in this thesis is the dissertation thesis of Najmanová. The author elaborated current findings in evacuation of preschool children of age 3 to 6 years to a form which can be further utilized in other engineering applications, mainly the fire safety engineering. The author conducted an elaborate research on state-of-the-art knowledge in evacuation of children, executed 15 experimental evacuation drills involving 970 children aged 3-6 in 10 nursery schools. The video recordings were analyzed to evaluate the evacuation phases and characteristics of children during evacuation. Furthermore, an online questionnaire of 20 questions was distributed to almost 5000 nursery schools in Czech republic. All of this allowed to form 18 behavioral statements on children behavior [7], some of which were utilized in the research of this thesis.

A close discussion with the author was happening about the requirements of the hierarchical model in this thesis to capture the specific behavior of children and make it fit to the new findings from the dissertation thesis. The focus was put on the basic principles of children's behavior and teachers' activities during evacuation as can be seen in real life situations. These principles were transformed to several strategies of the leading and following pedestrians together with behavioral rules.

Another key aspect of the model is the idea of hierarchical system of multi-agent coordination as developed by Janovská in her bachelor thesis [25]. The author developed a model of controlled swarm of agents, where agents had different roles. Leading agents, typically fewer in number, were responsible for controlling their group of following agent to the exit. The following agents, typically numerous, were less informed. The hierarchical structure of the two agent types was chosen to model the evacuation of school, where leading agents represent teachers and following agents represent children. The navigation of the leading agents was controlled centrally to minimise the loss of children and optimize the flow of the evacuation. The following agents were controlled reflexively.

The model in this thesis is composed of leading agents, which obey the strategies and rules of the central planning system, and following agents that are controlled reflexively based on their surrounding. The hierarchical model is following the principles of extended floor field model developed by Šutý [31], which offered a robust framework for modeling wide range of environments while keeping the computation requirements low.

Analysis and design

2.1 Hierarchical model

This thesis proposes a novel hierarchical system for the coordination of multi-agent evacuation simulations in a preschool environment. The hierarchical structure is a crucial aspect of the model, as it facilitates the efficient management of the various agents within the simulation highlighted in the work of Janovská [25]. The proposed system consists of two distinct agent types: following agents (followers) and a leading agent (leader). The following agents have the capability to form pairs and follow the orders of a leader, while the leader is responsible for navigating towards the goals and influencing agents in its close proximity. Additionally, both agent types can have varying speeds of movement to reflect real-world behavior. A centralized planning approach is employed to control the formation of pairs, the location of the leader in the queue, and the assignment of goals among others. The model presents a unique and innovative approach to the simulation of multi-agent evacuations in a preschool setting, which has significant implications for the field of emergency management and preparedness.

2.1.1 Floor field model

The baseline for the evacuation model with leading and following agents is a widely used extended cellular automata floor field model [32]. A cellular automaton (CA) is a mathematical or computational system composed of discrete elements (cells in Moore neighbourhood for a single agent and in extended Moore neighbourhood for a pair, further details in Section 2.2.8) that can be in a finite number of states. These elements are stochastically updated according to a set of rules. The variance in results due to stochastic selection can mimic the randomness observed in human behavior, making it a desired feature of the model. The floor field CA model, which is the inspiration for the model used in this thesis, utilizes several floor fields, including static, dynamic, and leader proximity, to model pedestrian movement in a two-dimensional lattice. Agents, representing pedestrians with individual parameters, move on the lattice and interact with the floor fields. The model update rules include updating the dynamic field, calculating the transition probability for a move to a neighboring cell, choosing a random target cell based on the probability, re-



Figure 2.1: Map `small.txt` initialized.

solving conflicts when two or more agents attempt to enter the same cell. The evacuation model in this thesis represents people in evacuation as agents who move on a rectangular two-dimensional grid that acts as a room, corridor or other area.

2.1.2 Hierarchical structure

The hierarchical system follows the research of controlling swarm with leading and following agents [25]. Such a system suits the environment of pre-school, where children (following or follower agents) are used to following a teacher, parent or other adult person with authority (leading or leader agent). The leading agent follows the optimal path (set by static floor field) to the current goal and sets the static floor field for the goal of following agents. At the same time, the leading agent can change its position in the crowd and influence the following agents by its proximity. More details are in Section 2.3.3. Leading agent takes into consideration following agents that are left behind and adjusts its speed to allow them to catch up. Also, following agents are semi-autonomous which means that they can evacuate the room when given the opportunity of being close to the exit.

2.1.3 Planning

Through communication with fire engineering expert H. Najmanová, the fundamental principles of children's behavior and teachers' activities during evacuation have been translated into a set of simple rules and strategies for the leading agent. These rules, when implemented, have been shown to impact the course of evacuation in several ways. Firstly, the speed at which agents move is affected, which consequently results in different total evacuation time (TET). Secondly, the structure and coherence of the group of agents is influenced. Lastly, the microscopic behavior of agents, including the formation of pairs, is observed to change. This thesis provides further research for many ideas from the dissertation thesis of Najmanová [7]. The developed model provides a framework for assigning goals and different rules for leading and following agents. The goals are executed sequentially. The model evaluates the state of agents (for example their positions and distances between each other) and the rules alter their behavior (for example increase their speed, change location). Static assignment of goals and rules defined in each map was sufficient for the needs of the research in this thesis. However, the framework can be easily adjusted to process goals and rules in real-time, for example by analyzing the state of the evacuation and generating goals as needed. The model is able to capture the complex interactions that occur during evacuation processes, and provides a basis for analyzing the effectiveness of different evacuation strategies.

2.2 Methods

2.2.1 Static floor field

Each cell in the grid in the static floor field (SFF) holds the value of shortest distance to the goal. The value is pre-computed using breadth-first search (BFS) algorithm. Movement to non-diagonal cells has a price of 1 and movement to diagonal cells has price of $\sqrt{2}$. The values are not normalized, because implicit normalization is present in the calculation of probability of moving to next cell. Alternatively, the distance can be computed by other algorithms, e.g. novel approximate algorithm described in [33].

2.2.2 Occupancy floor field

Each cell in the grid can hold at most one physical agent (leading or following). The virtual leader agent does not occupy a cell even though its position is the same as the cells position. The occupancy floor field (OFF) is a Boolean matrix of the same dimensions as the room. The position of cells occupied by a physical agent hold *true* value, otherwise the value is *false*. The occupancy floor field is updated in each step of the model.

2.2.3 Attraction and sensitivity parameters

The selection of the next cell by an agent is influenced by both the agent's own state (sensitivity parameters, timestep, and partner agent), as well as the state of the agent's surroundings (the SFF of the cell, distance to the leader, occupancy of the cell, and obstacles in the corner). The agent computes the attraction of each cell in its surroundings using a mixed strategy based on the method proposed by Šutý [31] shown in Equation 2.1. The attraction of each cell is then normalized across all cells to compute the probability of selecting a particular cell from the set. The probability of an agent moving from cell x to cell y , denoted by $P(y \leftarrow x | N)$, is calculated based on two members, P_O and P_S .

$$P(y \leftarrow x | N) = k_O P_O(y) + (1 - k_O) P_S(y) \quad (2.1)$$

Specifically, $P_O(y)$ takes into account the occupancy of cell y and returns a normalized value in the range $[0, 1]$. On the other hand, $P_S(y)$ considers the static potential of cell y and guides the agent towards the exit, along with the diagonal motion indicator $D(y)$. Both P_O and P_S are normalized across neighboring cells from N .

$$P_O(y) = \frac{\exp(-k_S S(y))(1 - O(y))(1 - k_D D(y))}{\sum_{z \in N} \exp(-k_S S(z))(1 - O(z))(1 - k_D D(z))} \quad (2.2)$$

$$P_S(y) = \frac{\exp(-k_S S(y))(1 - k_D D(y))}{\sum_{z \in N} \exp(-k_S S(z))(1 - k_D D(z))} \quad (2.3)$$

The equation for computing cell attraction serves as the baseline for solitary agents moving to Moore neighborhood. When paired partner agents are involved, each agent computes the attraction of both cells in each maneuver. For instance, agent a_1 in cell c_1 , paired with partner agent a_2 in cell c_2 , computes the attraction of maneuver $m_1 \in M$ in the following manner: $A_1 = A(a_1 \rightarrow c_{1*})$ and $A_2 = A(a_2 \rightarrow c_{2*})$, where c_{1*} and c_{2*} represent the cells after the maneuver. The attraction of maneuver m_1 is then determined as $A(m_1) = \min(A_1, A_2)$, and the probability of selecting maneuver m_1 by agents a_1 and a_2 is given by $P(m_1 | a_1, a_2) = \frac{A(m_1)}{\sum_{m_i \in M} A(m_i)}$.

2.2.4 Conflicts

The finite number of cells in discrete rectangular grid results in conflicts when two or more agents attempt to enter the same cell. The winner of this conflict, allowed to enter the cell, is picked randomly with uniform probability for each participant. This deviates from the conflict solution in research of aggressivity of Hrabák[34], where winner of the conflict was the agent with highest aggressivity or a conflict happened where no winner was selected. The described method was omitted in this research because it would bring more variability and less readability in the scope of this thesis' research. The framework is ready to include the method if needed. Intuitively, the author would recommend to assign highest aggressivity value to the leading agent and lower aggressivity value or distribution of values to the following agents.

The conflicts, where only one agent is allowed to enter a cell, result in a cancellation of movement for the rest of agents, that will stay in their position in the next step. Consequently, these agents prevent the movement of bonded agents behind them. The principle of bonds was first presented in [35]. Agent create a bi-directional bond when agent a_1 wants to enter cell c_2 occupied by agent a_2 . Once a_2 moves to other cell, the bond allows a_1 to enter c_2 . The method, which cancels the movement and breaks cycles is described in Chapter 3.

2.2.5 Orientation of directed agents

The grid in this model is a rectangular lattice of square cells where the agents can move from one cell to another in 8 directions of Moore neighbourhood (see Figure 2.2) and in special cases of a maneuver of a pair to the extended Moore neighbourhood as defined in Section 2.2.8. The agent has 4 possible orientations - North, East, South, West - which

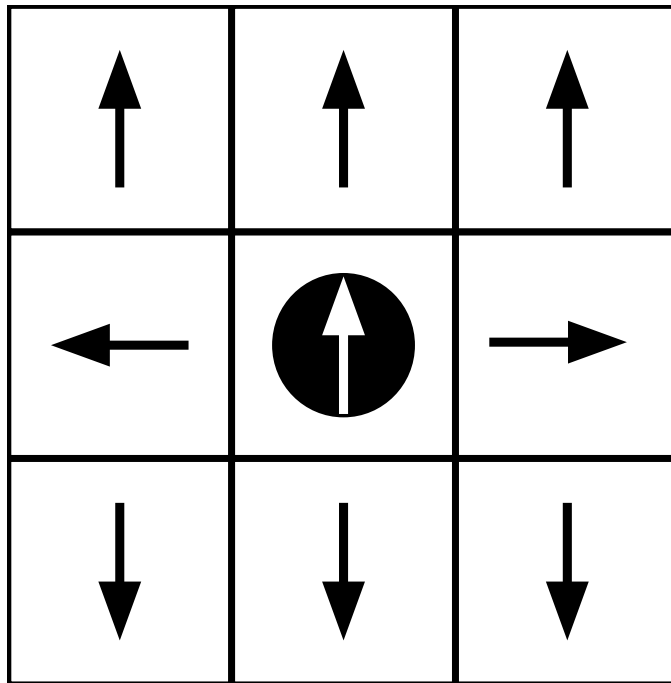


Figure 2.2: Directed agent is oriented to North. Arrows show resulting orientation after moving to cells in Moore neighbourhood.

are global and not relative to the agent itself. North represents the top of the grid and South the bottom, East is the right-hand side of the grid and West is the left-hand side. Even though the movement is possible in 8 directions the agent has only 4 orientations to facilitate the structure of paired agents. Two agents in a pair have the same orientation and are located in adjacent non-diagonal cells.

Directed agents take into consideration the direction of the movement. Moore neighbourhood allows movement in 4 non-diagonal and 4 diagonal directions. In case of the non-diagonal directions, the agent orientation after the move is the same as the direction of the movement: e.g. agent with orientation North moving to adjacent cell on the right will change orientation to East. In case of diagonal directions there are 2 types of movements: the first is movement to diagonal cells where the steering angle is +45 degrees and the second is movement to diagonal cells where the steering angle is +135 degrees. In the case of the movement to diagonal cell of the first type, the agents keeps his orientation unchanged, e.g. agent facing West moves to diagonal upper left cell will have West orientation after the movement. In the case of the movement to diagonal cell of

the second type, the agent changes the orientation to the opposite orientation e.g. North to South and vice versa, East to West and vice versa. The change in orientation after movement is depicted in Figure 2.2, where directed agent oriented to North can move to cells in Moore neighborhood. However, there are a few exceptions for paired agents as described in detail in Section 2.2.8.

2.2.6 Partner agents

Partner agents form a pair of two directed agents that are tightly bonded so that they are in adjacent cells to each other. Such formation follows the findings of Najmanová:

“...children form very often pairs holding each other’s hand (see the part focused on organisation of children in Section 6.3.3). In such organised formations, the process of overtaking is highly restricted and travel speed of individuals is limited not only by density conditions but also by the movement of children in front of them. Therefore, a splitting of a group into more subgroups and a subsequent waiting for the slower part of the group may be no exception.” [7]

Two partner agents in the pair cannot be in cells diagonal one to each other. Their movement is synchronous, which means that if any of the agent is not able to move to the desired cell (conflict, bonded agent did not move), the partner agent will abort its movement. The Algorithm 2 checks whether both agents will successfully move and if not, it cancels their movement and propagates the information down to all bonded agents. In this model, the two agents in the pair are in a hierarchy of one agent being the leader (not to be confused with leading agent which represents a teacher) while the second agent is not. The leader is responsible for calculating the probabilities of movement to cells for itself and its partner according to maneuvers. The leader is the agent which has its partner on the right. A pair of partner agents is depicted in Figure 2.4, where leader is colored black and its partner is colored white. The partner agents are directed agents and both have the same orientation. Note that some maneuvers change the leadership in the pair, see Section 2.2.8.

2.2.7 Pair formation

The children in pre-school age are being taught to form a pair and hold hands when walking through corridor or crossing a road as these situations pose risks such as getting lost or encountering traffic.

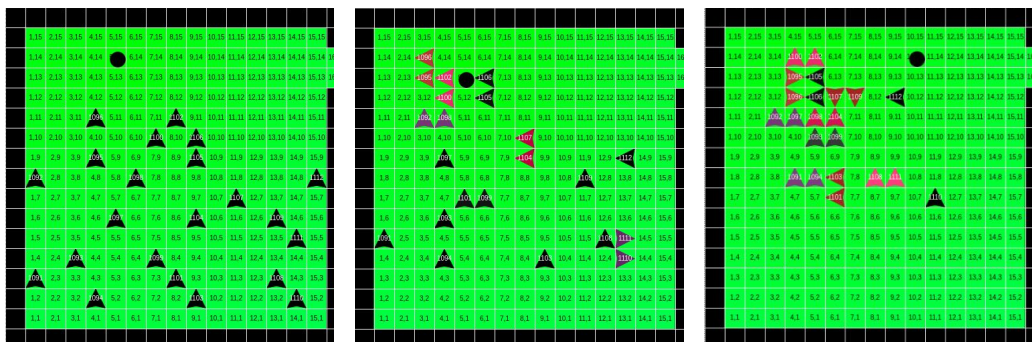


Figure 2.3: Example of pair formation in few steps of simulation. Initial positions of directed agents are on the left. The middle figure shows first paired agents. The right figure shows all agents formed in pairs apart from the isolated agents.

The agents (children) are located in a classroom in a cluster where some agents are close to each other and others are more isolated. The model does not consider any friendship preferences between children and assumes that agents close to each other are more likely to form pairs. It also assumes that agents form pairs in group of even number of agents so that there are no solitary children. If a agent can't form pair immediately it will do so when other solitary agent is nearby.

The process of forming pairs is shown in Figure 2.3, where at first no agents are in pairs, later some agents form pairs and in the last picture all agents apart from isolated agents are paired. The two agents in pair have same color.

Algorithm 1 Finding pairs

```

1:  $G = (V, E)$ 
2: while  $\exists v \in V : \deg(v) > 1$  do
3:   Let  $v^* \in V : \deg(v^*) = \max_{u \in V} \deg(u)$ .
4:   Let  $w \in V : \deg(w) = \max_{(v^*, w) \in E} \deg(w)$ .
5:   Remove  $(v^*, w)$ .
6: end while
7: for  $(v, w) \in E$  do
8:   formPair(v, w)
9: end for

```

The Algorithm 1 finds a way to form pairs of agents which are not yet in pair. Locations of solitary agents (directed agents) not in pair are transformed to a graph. The vertices of the graph correspond to the agents' locations, and an edge is formed between two vertices in adjacent cells. The vertices in the graph may have different degrees, and cycles may be present. The algorithm iteratively selects the vertex with the highest degree and removes the edge connecting it to the vertex with the highest degree until all vertices have at most one edge. The vertices connected by an edge represent a pair.

The pair formation is active during the whole simulation, so the model tries Algorithm 1 to pair any solitary agents.

2.2.8 Maneuvers

Each agent in a pair has the potential to move to 8 cells in the Moore neighbourhood and the combination of the movements create a vast number of possible maneuvers. However, most of these maneuvers do not maintain the structure of the pair and are therefore prohibited. Specifically, only 18 viable maneuvers are allowed for each orientation of the paired agents. They are various rotations and different directions of maneuvers shown in Figure 2.4 and 2.5. The definition of these maneuvers was discussed with the fire engineer expert to express the characteristic movement of children in pairs and allow a natural movement of the paired agents in corner.

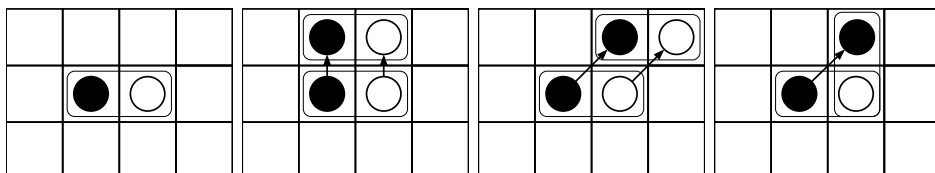


Figure 2.4: Simple maneuvers of paired agents that do not change leadership. Leader in the pair is painted black.

Some maneuvers can alter the leadership of the pair or the orientation of the agents as is depicted in first three schemes in Figure 2.5, where the leader in a pair colored black loses its leadership and is colored white. The change of leadership is essential to preserve the structure of a pair.

Additionally, in some cases, the agents may have different movement speeds. During the synchronous atomic movement of a maneuver, both agents may move to diagonal cells, or one agent may move to a diagonal cell while the other remains in its current cell. In the Figure 2.5, the last scheme shows the maneuver, where black agent moves outside its Moore neighborhood in order to preserve the structure of the pair. The agent in the movement moves over three cells but the time duration of the maneuver is only double. This movement pattern results in more natural turning.

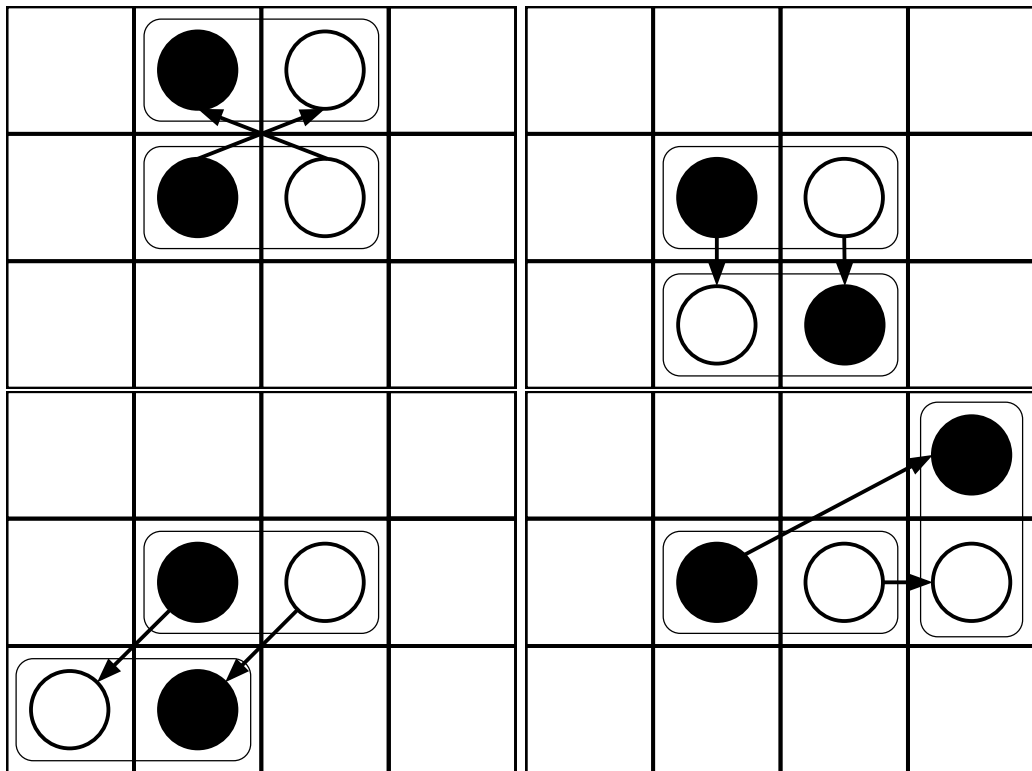


Figure 2.5: Complex maneuvers of paired agents that change leadership. Leader in the pair is painted black.

2.2.9 Leading agent and virtual leading agent

The solitary agent responsible for navigation is the leading agent, which has complete information about the map topology and goals. The leading agent is not a directed agent and can't form a pair. It selects the optimal cell in the Moore neighborhood for next move. The virtual leading agent is a leading agent, which does not occupy a cell but virtually moves in the grid. The SFF for the (virtual) leading agent differs from the SFF of follower agents. The (virtual) leading agent SFF navigates to the current goal while abiding to strategy (for example position at the back of the crowd or standing guard at a location). In case of different position of leading and virtual leading agent in the crowd, these two have different SFF.

The Figure 2.6 shows a leading agent (black circle) at the end of the crowd and a virtual leading agent (white circle) at the front of the crowd. The SFF of followers is depicted by green for low values and blue for higher values. It is centered around virtual leading agent. The SFF for virtual leading agent (not shown) navigates towards the exit

2. ANALYSIS AND DESIGN

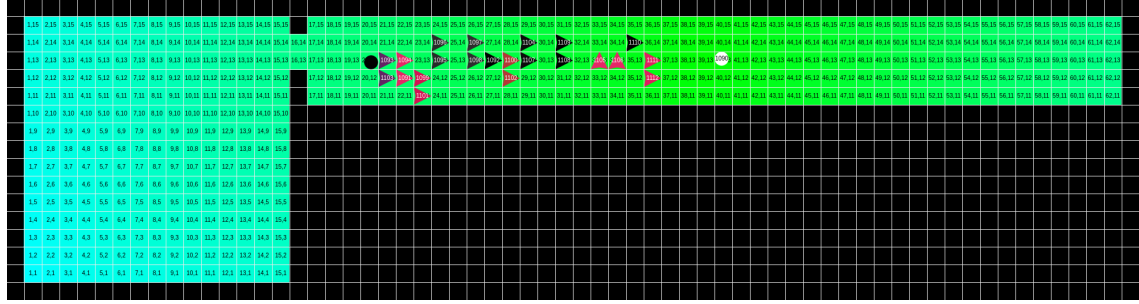


Figure 2.6: Virtual leading agent (white circle) sets SFF with its location as goal. Leading agent (black circle) is positioned at back of the crowd.

at the end of corridor. The SFF for physical leading agent (not shown) is centered around the end of the corridor. This visualization is not present in the current model. Currently, in the visualization the virtual leading agent is not visible and the visualized SFF is the SFF of the exit.

The virtual leading agent is always located at the front of the crowd and navigates the followers when the leading agent moves to the end of the crowd or it is standing guard at a location. The follower agents, solitary or in pairs, follow the SFF set by virtual leading agent location and they do not attempt to find their own way to the exit, which is similar to children behavior in evacuation [7]. The SFF for follower agents is calculated in every step based on the virtual leader’s position.

Agent’s proximity to the leading agent (not virtual leading agent) proportionally increases the static potential value by increasing the sensitivity to static potential k_S :

$$d = \text{distance}(\text{leader}, \text{follower})$$

$$k_S = k_S * (1 + \frac{1}{d})$$

With a higher sensitivity to static potential, the agent is less likely to deviate from the optimal trajectory set by the SFF of the virtual leader. This method is described in more detail in Section 2.3.3. The leader has simple rules for navigating towards the closest goal and checking if all follower agents reached the goal. One rule is the leader’s ability to command the follower agents to continue to the goal while the leader moves to the most distant agent. Additionally, the (virtual) leader agent waits near the goal area and attracts the follower agents until they all reach it.

2.3 Strategies and rules

The model uses strategies and rules to capture the specific children behavior during evacuation, which Najmanová described in [7]:

“Based on the leaving strategy employed, the following situations were observed during the experimental evacuation drills:

1. *Leaving as a group at once: All children were gathered in front of a closed exit from a classroom forming a standing queue, first the whole group was completed the door was opened and children started to leave the classroom.*
2. *Leaving as a group gradually: All children were leaving together, however they were not gathered and checked in front of an exit from a classroom but when they arrived at the door as a moving queue, the door was already opened and supervised by a staff member and they could leave the room smoothly.*
3. *Individual leaving: Even though supervised children could leave a classroom individually instructed to wait at a specified place inside or outside the building.”* [7]

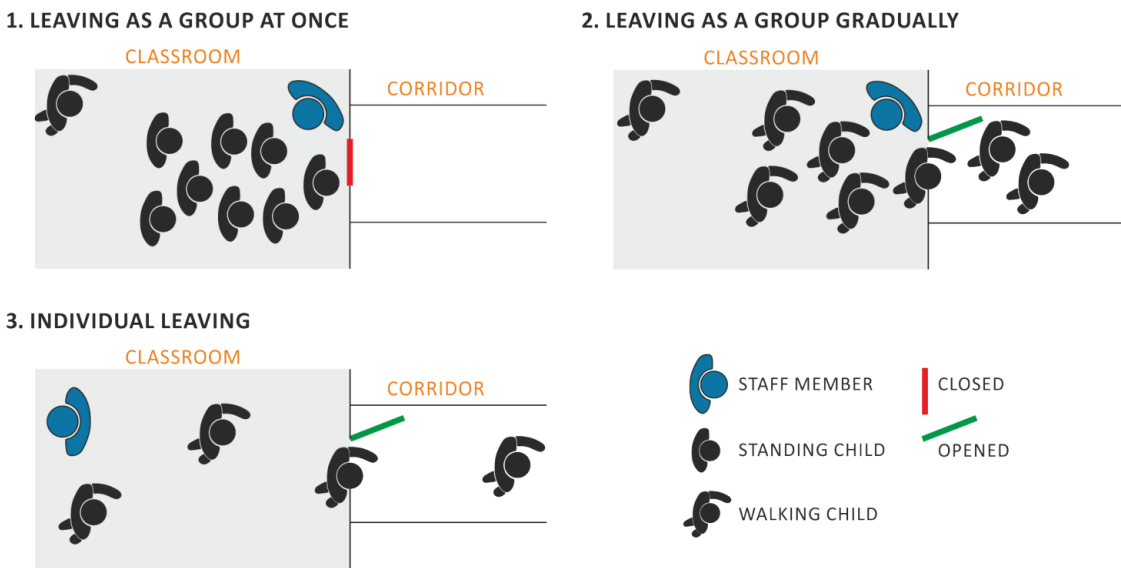


Figure 2.7: Visualization of specific children behavior during evacuation. Image taken from [7].

2.3.1 Leading agent strategy

In the hierarchical system a leading agent is responsible for navigating the following agents. The leading agent can achieve it in different ways as defined by the strategy. There are three leading agent strategies:

- (A) Navigate towards the exit and evacuate.

Leading agent follows the optimal path to the exit. Leading agent is positioned at the front of the crowd, the following agents are navigated by SFF calculated for them by virtual leader which has same position as the leading agent. Any agent, including the leading agent, that reaches the exit evacuates the room immediately.

- (B) Navigate towards a location with specific position of the leading agent in the crowd.

Virtual agent follows the optimal path to the location. The leading agents position can be at the front or at the back of the crowd. The role of a virtual leader is essential in this strategy because the virtual agent is always at the front of the crowd and sets SFF for following agents. The virtual leader agent dynamically evaluates the distance to the most distant following agent and adjusts its own speed (and the speed of the leading agent if positioned at the front) so that the distant agent is not left too far behind. In the case of a leading agent positioned at the back of the crowd, leading agent adjusts its speed dynamically so that it is always at the back of the crowd. For detailed explanation visit Section 2.3.4. The close proximity of the leading agent at the back of the crowd increases the speed of the following agents at the back of the crowd so that they could catch-up with the crowd and make it more compact. In the end, the virtual agents tries to make the crowd compact by adjusting the speed at the front and the leading agent at the back influences the following agents at the back to make the crowd more compact.

- (C) Leading agent standing guard at a location and following agents navigate towards next goal location.

Leading agent is standing at a strategic location, for example next to the exit or at an apex of a corner and the following agents are navigated by SFF set by virtual leader to their goal location. Following agents in the crowd pass the leading agent at a close proximity and adjust their speed within the crowd due to its influence. The leader joins the crowd at the back.

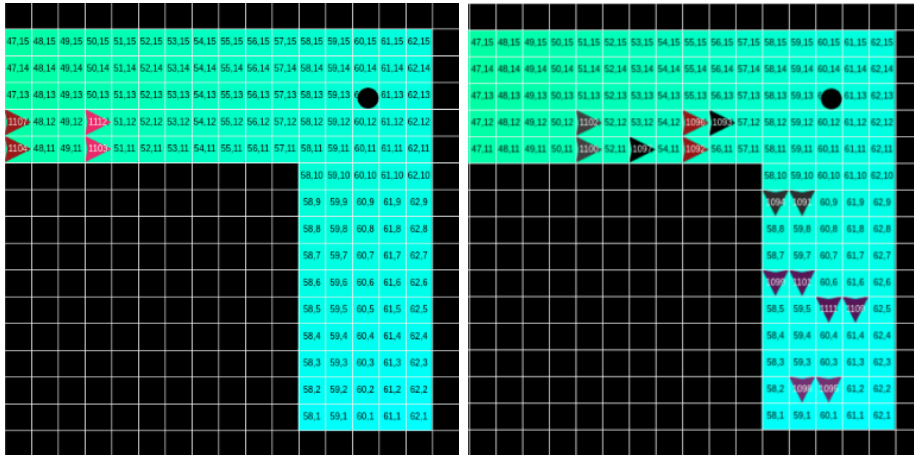


Figure 2.8: Leader strategy standing guard at a location and waiting (left), following agents passing the leader and navigating towards goal (right).

2.3.2 Breaking pairs

The model implements the movement of paired agents through atomic and consistent maneuvers, preserving the structure of a pair. However, when paired agents approach a congested exit cell, their movement maneuvers become challenging due to high cell occupancy in the area of the exit. To overcome this difficulty, the pairs are split when they are in close proximity to the exit, but not when they are near their current goal. It is noteworthy that the topology of the map assumes a suitable path and adequately wide corridors to accommodate paired agents, thus eliminating the need for methods to handle dynamic breaking and creation of pairs based on the current evacuation status. Nonetheless, the

framework can be customized to cater to specific requirements, as dynamic creation or breaking of pairs is already incorporated into the model and can be easily modified.

2.3.3 Penalization and discipline

The behavior of children is known to be strongly influenced by the presence of authority figures, such as parents, teachers, or other responsible adults. In the proposed model, the leader assumes the role of authority and guides the children as they move through the environment. Specifically, children who are in close proximity to the leader exhibit higher levels of *discipline* and move in a more orderly manner, preserving the structure of the queue of pairs and following the optimal path as determined by the SFF. To promote this behavior, the static force value assigned to each agent is adjusted according to their proximity to the leader. In particular, as the distance d between an agent and the leader decreases, the sensitivity to SFF k_S assigned to that agent is multiplied by a factor of $(1 + \frac{1}{d})$. By moving back and forth within the queue, the leader can selectively increase the discipline of agents in close range and have greater control over the overall behavior of the group.

The paired partner agents form a queue and move one pair after other. Due to the nature of *maneuvers* described in Section 2.2.8 the paired agents sometimes rotate and change orientation because a non-optimal maneuver was selected stochastically. To limit this behavior a penalization for maneuvers with incorrect change of orientation is introduced. The penalization value can be set to fit needs of the simulation. Every maneuver which results in unwanted change of direction is multiplied by the penalization and consequently there is a lower chance of it being selected.

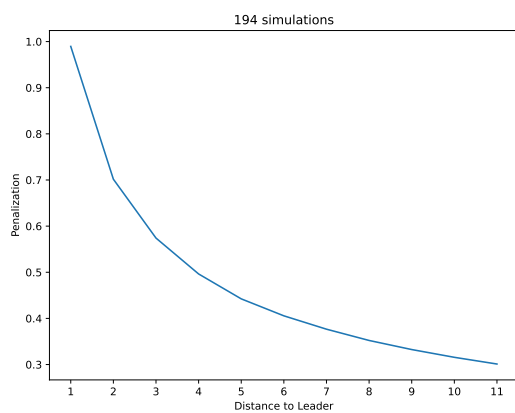


Figure 2.9: Penalization decreases with distance to the leader.

Maneuvers, that turn the pair are wanted in case of agents turning in corner. The correctness of the orientation is thus determined by the orientation of the most attractive maneuver. The two examples in Figure 2.10 show how a correct orientation is selected. On the left, the paired agents facing North follow the leader which leads them to the North. The attractivity of maneuver moving both agents to the North is the highest and thus the correct orientation is North and maneuvers resulting in different orientation are penalized. On the right example, paired agents facing East approach a right-turn in corridor where leader passed the turn and is located on the South. The maneuver which results in rotation of the agents to the South is the most attractive and thus the orientation South is selected as correct and maneuvers resulting in different orientation are penalized. Further examples of penalized and non-penalized maneuvers are present in Figure 2.13.

The influence of penalization of maneuvers resulting in incorrect orientation is seen in the Figure 2.11, where the graphs show ratio of selected maneuver with incorrect orientation compared to ratio of all maneuvers in relation to distance to leader. The yellow dots show the ratio of maneuvers selected at the distance to the leader on x axis. The blue line shows how many of the maneuvers at the specific distance resulted in incorrect orientation. The graph on top shows simulation with penalization value 1. At small distance to the leader a low proportion of maneuvers resulted in incorrect orientation and

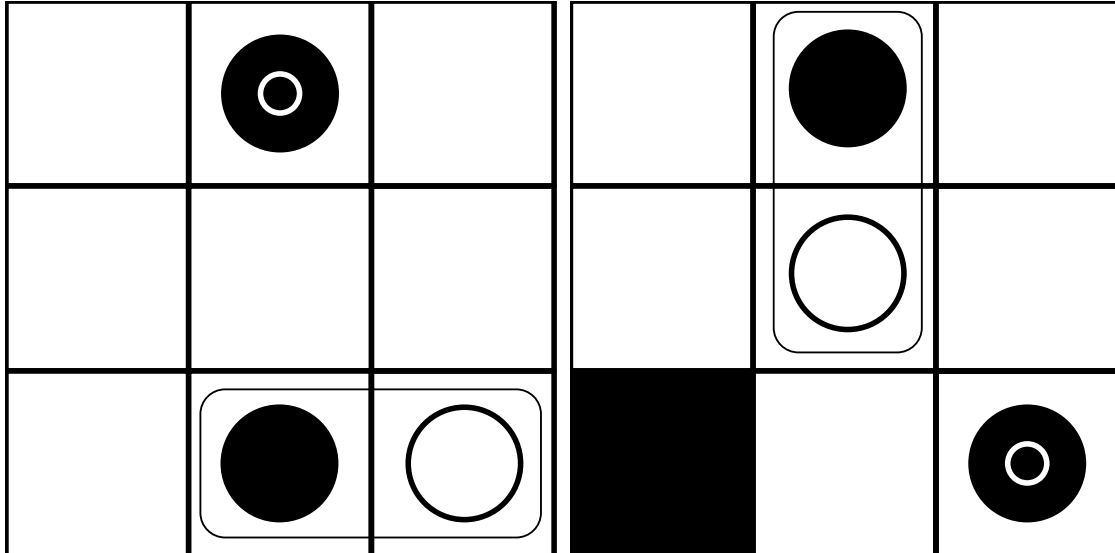


Figure 2.10: Two situations where a different correct orientation is selected based on the position of the leader, which is colored black with smaller white circle inside. On the left, the maneuvers for paired agents directed to North which result in North orientations are not penalized. On the right, the leader passed the corner and the paired agents should turn to South. Maneuvers resulting in other orientation than South are penalized.

the number increases with distance to the leader. The graph on bottom shows simulations where penalization had value 0, which means it had no effect on the maneuver selection. It can be seen, that at every distance to the leader, little below 30% of maneuvers resulted in incorrect orientation.

The nature of discrete rectangular grid lowers the resolution of movement around obstacles which needs to be addressed. A obstacle crossing penalization is introduced, which aims to restrict diagonal movement of agents across obstacles. An example of agent crossing an obstacle is shown in Figure 2.12.

The degree of penalization may be customized based on the requirements of the simulation, with a value of 0.5 being adopted in this instance. Non-obstacle crossing maneuvers do not incur any penalty. The degree of attraction is scaled by the penalization factor, with higher penalization values resulting in less obstacle-crossing maneuvers. Lower penalization of crossing penalization maneuvers in environments with narrow corridors or numerous obstacles can result in smoother movement of paired agent queues.

2.3.4 Adaptive speed

This model allows agents to adjust their movement speed during an evacuation, with the leader represented as an adult with an average speed of $1.2m/s$, as per the findings in [2]. Follower agents, who are modeled as children, are assigned a speed of $0.9m/s$, based on experimental measurements of children walking speed which ranges from $0.84m/s$ to $1.6m/s$ per findings described in [7]. Each model step consists of two timesteps. Timestep represents the unit duration of movement. The method of time using timesteps was described in [36]. For instance, paired agents have a movement duration of three timestep units with a speed of $0.9m/s$, resulting in a speed of $0.3m/timestep$. The leader agent has a speed of $0.4m/timestep$. This update frequency of two timesteps per model step allows for synchronization of movement every three steps between the leader agent and paired agents.

Specifically, each agent is equipped with an internal counter, denoted by τ , which is evaluated against the model's timestep clock, denoted by T . The timestep clock T

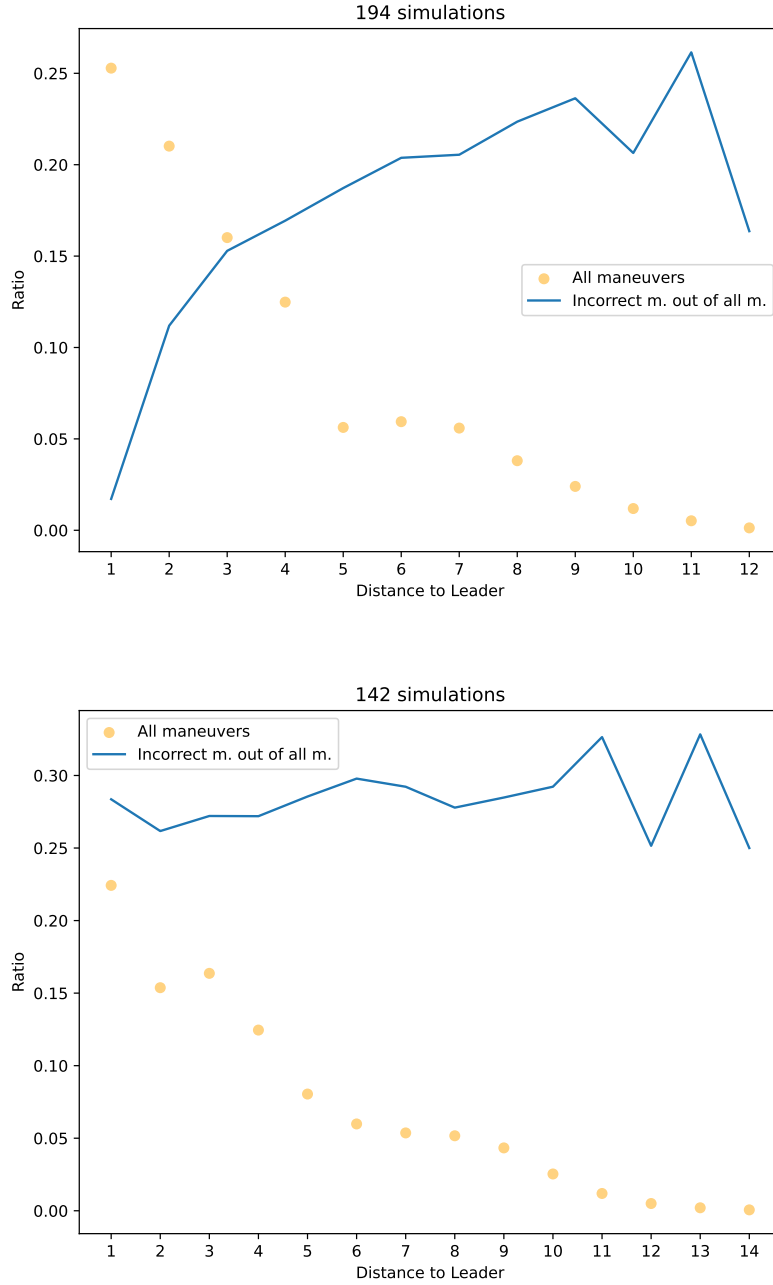


Figure 2.11: Simulations with penalization value 1 in the top figure show few incorrect maneuvers compared to bottom figure where penalization is 0.

advances by two timesteps for each model step. Filtering timed-out agents is done by condition $\tau > T$. The rest of the agents that fit below T can initiate cell selection and increment τ by the duration of the maneuver if they move.

Paired agents can dynamically adapt their speed in specific conditions. Close proximity to the leader and empty cell in front of them increases their speed. The leader agent can move back and forth in the queue and locally increase the speed of paired agents to repair the queue structure or close the gaps between agent pairs. The change in speed reverts when previous conditions are not met. The leading agent, modeled as an adult person, has higher speed than following agents. For n following agents in the simulation, the model calculates distance from the virtual leading agent (at the front of the crowd) to

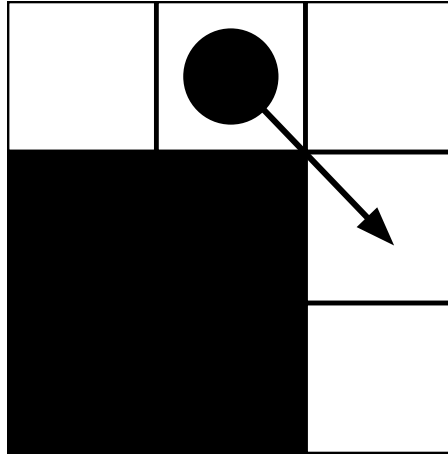


Figure 2.12: Agent crosses an obstacle. This movement is penalized, although possible.

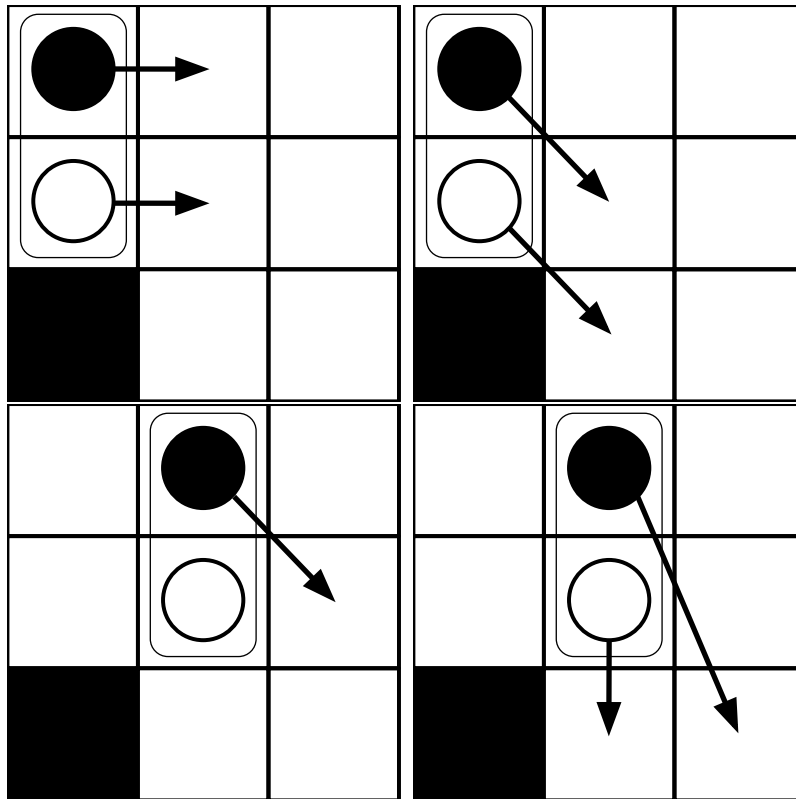


Figure 2.13: With exit placed at the South, the simple maneuvers on the left are not penalized. The diagonal maneuver in the top right results in correct orientation but the white agent is passing an obstacle thus obstacle penalization is applied. The complex maneuver in the bottom right is not penalized but black agent τ is increased with twice the movement duration.

the most distant agent d and lowers virtual leading agents speed when $\frac{n}{2} \leq d$. In case of leading agent at the back, the distance d is calculated from the leading agent to the agent at the back. When $d < 5$, the leading agent keeps its current speed, otherwise its speed is increased to catch up with the crowd. The leading agent being very close to the slow agent at the back of the crowd increases the speed of the slow agent to catch up with the rest of the crowd, shown in Figure 2.14.

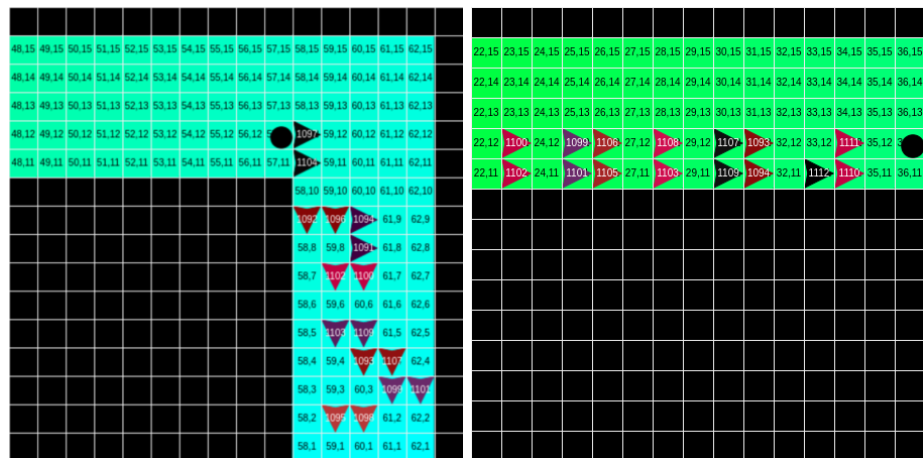


Figure 2.14: Leader position at the back (left) and at the front of the crowd (right).

Implementation

The implementation of the model framework was carried out in Python, version 3.10, using several accompanying libraries. The complete source code is accessible at <https://gitlab.fit.cvut.cz/sutymate/mt-master-thesis>, along with comprehensive documentation and installation guidelines. The maps, an integral component of the model, are also included in the repository.

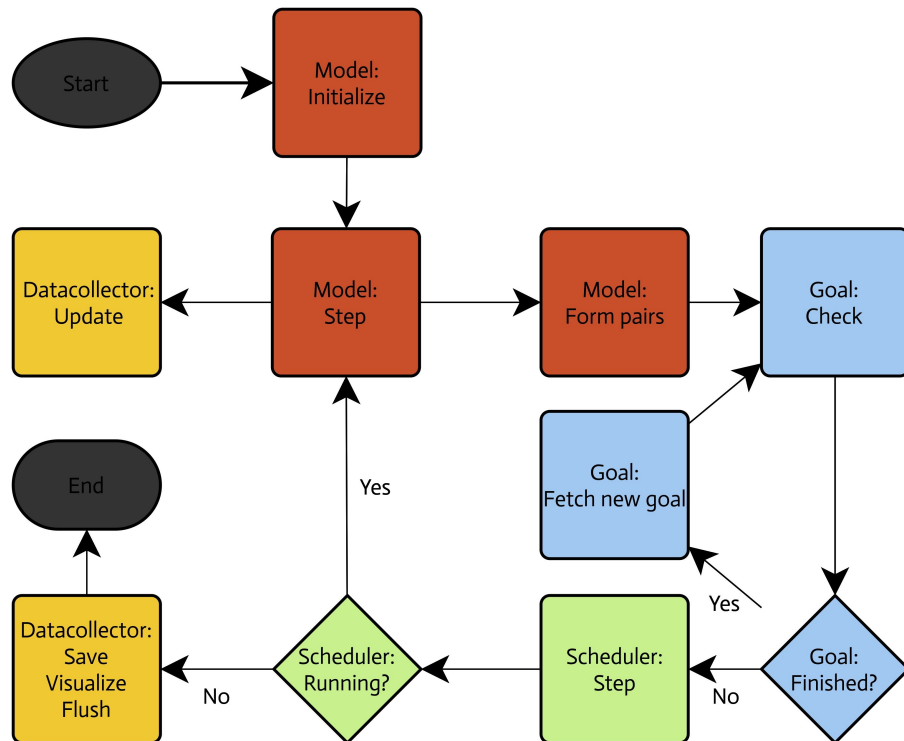


Figure 3.1: Schema of one simulation run.

In short, the architecture of the model is made out of several objects resting in the *RoomModel* class. *RoomModel* orchestrates initialization of the model, running it, collecting and saving data, creating graphs. The sequence is depicted in Figure 3.1. *SequentialActivation* is a scheduler of agent movement in the cells. As can be seen in the Figure 3.2, the sequence starts by selecting agents that have $\tau < T$ as described in Section 2.3.4. These agents calculate *attractiveness* of the cells in their neighbourhood and stochastically select their desired cell. Next, the cells which are selected by agents for entrance execute winner selection, which means that they select the agent from all candidates that want to enter the cell. Next, all participating agents verify whether they will enter their desired cell. If so, they will update their τ with the duration of the movement. If they can't enter

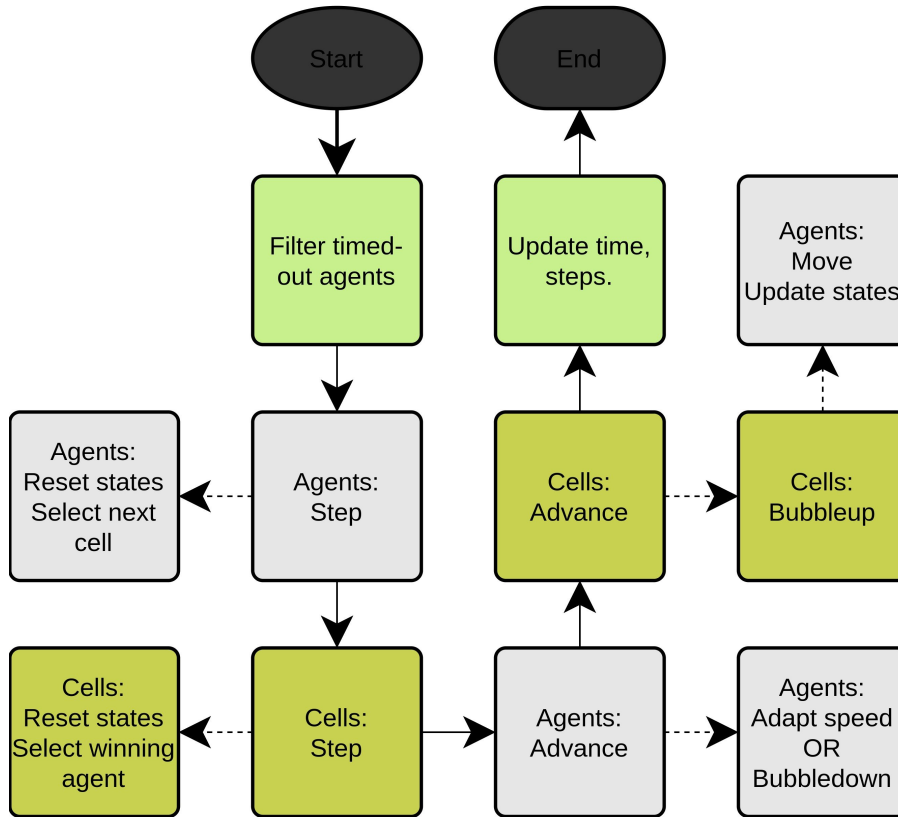


Figure 3.2: Task flow in one step of *SequentialActivation* object.

their desired cell, they will *bubbledown* the information to bonded agents behind them and cancel their movement as they won't move from their position, see Algorithm 2.

Algorithm 2 Agent bubbledown method

```

1: function BUBBLEDOWN(AGENT)
2:   if agent.next_cell.winner == agent then
3:     agent.next_cell.winner ← null
4:   end if
5:   agent.next_cell ← null
6:   agent.confirm_move ← false
7:   if agent.partner.next_cell ≠ null then
8:     bubbledown(agent.partner)
9:   end if
10:  if agent.head ≠ null then
11:    agent.head.tail ← null
12:    agent.head ← null
13:  end if
14:  if agent.tail ≠ null then
15:    agent.tail.bubbledown()
16:  end if
17: end function
  
```

Next, the cells with winning agents *bubbleup* the bonded agents to the front of the bond chain up to the agent which: a) has empty cell to enter, b) the chain of bonded agents forms a cycle, which is detected and broken, see Algorithm 3. An example of trivial cycle of bonded agents is shown in Figure 3.3, where three agents want to move to cell indicated

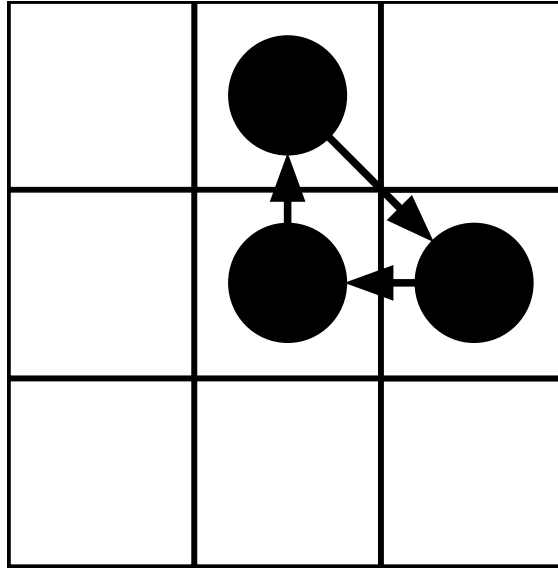


Figure 3.3: Three agents form a cycle, which is detected and broken. The arrows indicate their desired cell in the next move.

by an arrow. In either case, the agents participating in *bubbleup* will successfully move to their desired cell. Lastly, the scheduler updates internal states such as number of steps and timestep value.

Algorithm 3 Cell bubbleup method

```

1: function BUBBLEUP(CELL)
2:   head  $\leftarrow$  cell.winner
3:   origin  $\leftarrow$  cell.winner
4:   while head.head  $\neq$  null do
5:     head  $\leftarrow$  head.head
6:     if head = origin then
7:       origin.head.tail  $\leftarrow$  null
8:       origin.head  $\leftarrow$  null
9:     end if
10:   end while
11:   return head
12: end function
```

3.1 Mesa

Mesa is a popular framework for ABM research [37]. The API offers many options for visualization, setting of parameters, data collection, etc. This framework has been successfully used in the previous research of SFF CA model of pedestrian evacuation in 2020 [31]. Moreover, Mesa was used in research of software for urban planning practice [38], multi-drone truck routing problem [39] and in the simulation of balancing consumer and business value of recommender systems [40].

3.1.1 Visualization

Mesa framework has built-in visualization module for web browser, which is suitable for fast development and visual analysis. The user can adjust the speed of simulation or continue step by step to watch in detail. Simulations can be rerun. Figure 3.4 shows the Mesa visualization in browser for a map *small.txt*. The black circle represents a physical leading agent, the two arrow agents of same color are paired agents with orientation to the West. The color gradient shows SFF of the exit. Black grid cells represent obstacles. The parameter interface is described in Section 3.1.2.

3.1.2 Run-time parameters

The user can better understand the simulation when it runs under various settings. Mesa offers a user-friendly interface for setting global parameters of the simulation. As can be seen in the Figure 3.4, user can set various parameters:

- Sensitivity to static field k_S , where higher value increases the attractivity of the optimal cells as can be deducted from the Equation 2.1.
- Sensitivity to occupied cell k_O , where higher value prevents the agent from selecting occupied cell for next move.
- Sensitivity to diagonal movement k_D , where higher value prevents the agent from selecting diagonal cell for next move.
- Movement duration for leader in timesteps, where higher value results in a longer duration of leading agent's movement and thus lower speed.
- Movement duration for followers in timesteps, where higher value results in a longer duration of following agents' movement and thus lower speed.
- Penalization for incorrect orientation, where higher value penalizes maneuvers resulting in incorrect orientation and lowers their attractivity.
- Switch for leader location at the front forces the agent to keep position at the front of the crowd. When the simulation follows goals defined in the map file, this setting will be overwritten by the goal rules.

After setting new parameters, the simulation needs to be restarted.

3.1.3 Definition of map and rules

The maps used by the model are defined in an ASCII text file and can be created or edited for user's needs. The model requires the following structure:

```
maps/
 - data/<map_name>.data
 - topology/<map_name>.txt
```

An example of the input file format used in the simulation is shown in Listing 3.1.3. The map itself is defined at the beginning of the file using `#` symbol to represent obstacle, empty space for empty space and various types of agents as follows: `L` for leading agent's positions, `D` for directed agents' positions, other symbols are deprecated. After the map topology definition follows a custom hash value (in example 42), which validates the map topology to the precomputed SFF values in `/maps/data/<map_name>.data`. After that follow sequentially the goals together with rules. As described in Section 2.3, there are three goal types:

- Navigate towards the exit and evacuate is indicated by `E` followed by x, y coordinates and keyword `All`.
- Navigate towards a location with specific position of the leading agent in the crowd is indicated by `L` followed by integer x, y coordinates. Then an integer t tells the leader how long to stay in the position after the goal was reached. Position of the leader is marked by keyword `Front` and `Back`. Keyword `All` ends the sequence.
- Leading agent standing guard at a location and following agents navigate towards next goal location is indicated by `G` followed by integer x, y coordinates of leading agent's location. Then an integer t tells the leader how long to stay in the position after the goal was reached. Position of the leader is marked by keyword `Front` and `Back`. Keyword `All` ends the sequence.

Listing 3.1: Example of map definition file.

```
#####
#   # LD #
#           D #
#   #   #
#####
42
G 7 3 0 Back All
L 2 2 0 Front All
E 1 2 All
```

3.1.4 Simulation experiments module

Simulation experiments are defined in the abstract class `Experiment`. `Experiment` provides interface to simply initialize simulation data in required format, load data from previous runs, update them with current run and save for later use. Also, each experiment defines how to visualize data.

3.1.5 Datacollector

`RoomDatacollector` class provides a simple interface for running multiple `Experiment` instances and saving, showing or just aggregating the data. At the same time, `RoomDataCollector` is a derived class from the Mesa `DataCollector` class, which can be used to visualize data in real time in the browser visualization.

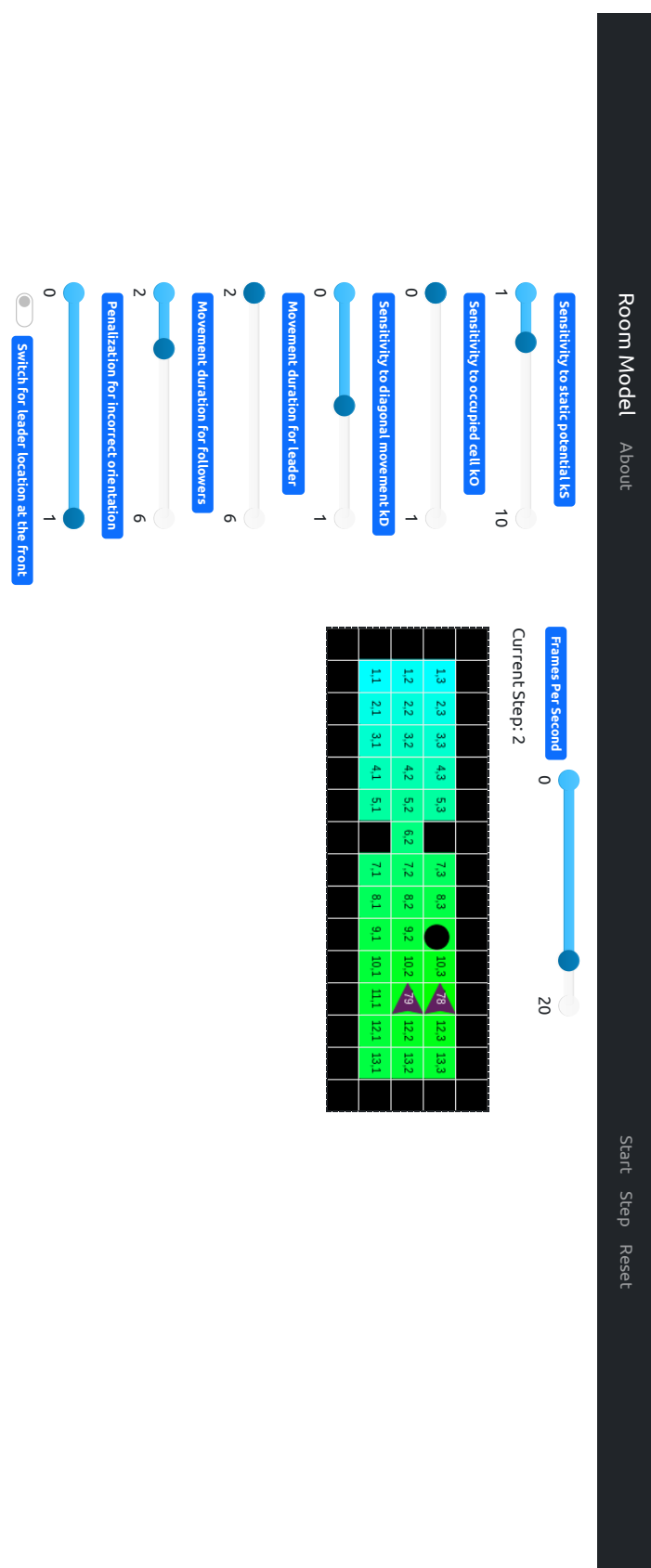


Figure 3.4: Visualization of evacuation simulation in browser.

Simulation experiments

4.1 Maps

In the simulation experiments, four distinct map files were utilized. The first three maps, `mapX1.txt`, `mapX2.txt`, and `mapX3.txt`, each featured a classroom setting with varying corridor lengths and shapes. `mapX1.txt` had a long corridor, while `mapX2.txt` had a shorter corridor. `mapX3.txt` included a turn in addition to the short corridor, making it slightly more complex than the other two maps. The first two maps have exit location at the end of corridor. Locations *A*, *B* are the same for all three map types with classroom. The most complex map `mapX3.txt` has a location *C*, which shows the guarding location of leading agent. The fourth map file, `gapsX.txt`, depicted a narrow corridor with trigger gates. For clarity, the classroom maps are depicted below in Figures 4.1, 4.2, and 4.3, while `gaps.txt` is shown in Figure 4.4. Overall, the selection of these four maps allowed for a diverse range of scenarios to be simulated and tested.

Simulation experiment runs with different goals and strategies are described in the Table 4.1.

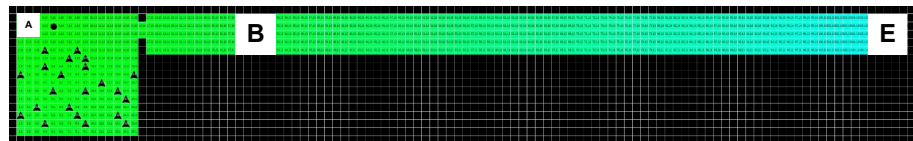


Figure 4.1: Initial positions and goals of leading and following agents in the classroom `mapX1.txt`.

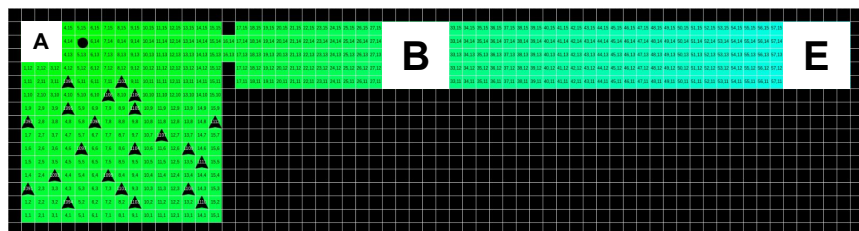


Figure 4.2: Initial positions and goals of leading and following agents in the classroom `mapX2.txt`.

Table 4.1: Goals of each map

Map	# of Agents	Goal 1	Goal 2	Goal 3	Goal 4
map01.txt	22 + 1	Exit (Front)	Location B (Front)	Exit (Front)	
map02.txt	22 + 1	Location A (Front)	Location B (Back)	Exit (Back)	
map03.txt	22 + 1	Location A (Front)	Location B (Back)		
map11.txt	22 + 1	Exit (Front)	Location A (Front)	Location B (Front)	
map12.txt	22 + 1	Location A (Front)	Location B (Front)	Exit (Front)	
map13.txt	22 + 1	Location A (Front)	Location B (Back)	Exit (Back)	
map21.txt	22 + 1	Exit (Front)	Location A (Front)	Location B (Front)	
map22.txt	22 + 1	Location A (Front)	Location B (Front)	Exit (Back)	
map23.txt	22 + 1	Location A (Front)	Location B (Front)	Guard C (Front)	
gaps.txt	8 + 1	Exit (Front)	Exit (Back)	Exit (Back)	
gaps_back.txt	8 + 1	Exit (Back)			

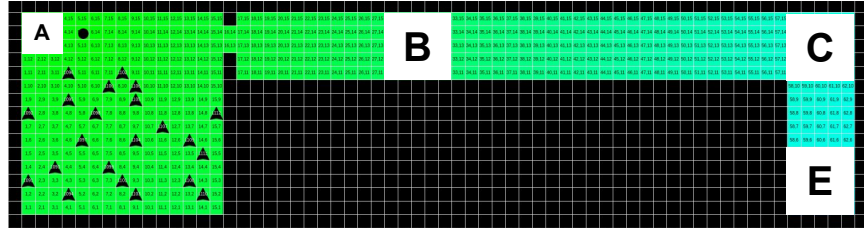


Figure 4.3: Initial positions and goals of leading and following agents in the classroom mapX3.txt.

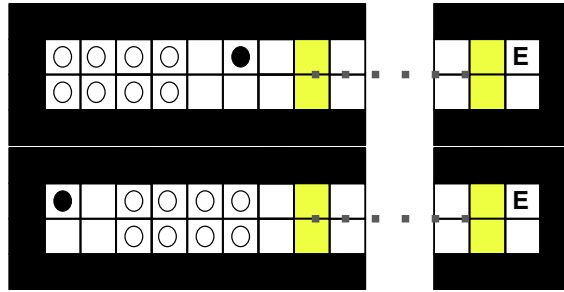


Figure 4.4: Illustration of maps gaps.txt on the top and gaps_back.txt on the bottom. Trigger points are depicted as yellow cells and dots show the cells that were hidden due to the length of the map.

4.1.1 Room size for simulation experiments

According to legislation outlined in the civil engineering law of the Czech Republic, a minimum of 1.65 m^2 of space per person is required during the educational process in pre-school classrooms, with a recommended corridor width of 2 meters and a minimum width of 1.2 meters. Doors must have a required width of 90 centimeters [41]. In 2019, the Czech Statistical Office released a report on pre-schools and other educational institutions, indicating that the average number of children in a pre-school classroom is 22.6 [42]. Subsequent research conducted by Najmanová in 2020 further supports this finding, revealing that the most frequent number of children in a class ranged between 20 and 28 children (80.1%) with a median value of 24 children [7]. For the purposes of simulation experiments, classroom dimensions are set to 15×15 cells with a door width of 2 cells and a corridor width of 5 cells. Assuming a cell size of 40 centimeters, commonly used in evacuation simulation CA models, the resulting classroom dimensions are 6×6 meters with a door width of 80 centimeters and a corridor width of 2 meters. With each child having approximately 1.63 m^2 of space in the classroom, the minor discrepancy between the required space per child and the space utilized in the simulation, resulting from differences in door width and resolution of the SFF CA model, is negligible [41].

There is also other map type gapsX.txt, which puts focus on the structure of a queue of pairs following leader and the selection of incorrect orientation maneuvers. These maps are narrow and long, with 2 cells in width and 60 in length. There are 8 directed agents and one leader, so that these agents could form pairs and follow the leader. The maps have trigger gates which initiate experiment of measuring distance between pairs at cell 11 of width and cell 40 of width, which ends the experiment.

Simulation experiment	k_S	k_O	k_D	Penalization	Leader	Pairs
Penalization low	3	0	0	0	Yes	Yes
Penalization middle	3	0	0	0.5	Yes	Yes
Baseline	3	0	0	1	Yes	Yes
k_O medium	3	0.5	0	1	Yes	Yes
k_O high	3	1	0	1	Yes	Yes
k_S low	1	0	0	1	Yes	Yes
k_S high	5	0	0	1	Yes	Yes
Leader, no pairs	3	0	0	1	Yes	No
No leader, no pairs	3	0	0	1	No	No

Table 4.2: Parameter values for simulation experiments

Results

The simulation experiments conducted using the proposed hierarchical model investigated various aspects of the simulated evacuation. One part of the simulation experiments aims to investigate the structure and behavior of paired agents following a leading agents. The results describe the gaps between pairs during the course of the evacuation, the consistency of their distance to the leader, the symmetry of the results based on the leader position in the pair and lastly the effect of the penalization parameter on the ratio of maneuvers resulting in incorrect orientation.

The model needs to be versatile to simulate evacuations in various environments and situations, which is investigated in the simulation experiments of the total evacuation time in different maps, scenarios and parameters. Additional analysis of specific flow of agents through key areas in the environment explain the dynamics of the simulation and the way scenarios effect it. The hierarchical model is based on the floor field CA model, which operates with several model parameters. The influence of the major parameters k_S and k_O , as noted in the sensitivity analysis [31], is analysed.

The analysis of the simulation experiments provided valuable insights into the pedestrian movement in the hierarchical model. The results shed light on how individual parameters impact the course of the evacuation and the structure of agent pairs. Additionally, the use of strategies and rules was closely examined to correspond to the behavior of child agents on qualitative level.

5.1 Gaps between pairs

The present study involves a simulation experiment conducted on the maps `gaps.txt` and `gaps_back.txt`, which feature a narrow long corridor with a leading agent (positioned at the front and at the back of the crowd) and eight following agents, as depicted in Figure 4.4. The Figure depicts two trigger zones in yellow that border the investigated area. When the following agents move in the investigated area they are already in pairs and the initial noise in pair formation is reduced as well as the noise at the exit. In each step of the model, the pair position is captured and later processed as a distance between pairs. It is important to note that the trigger zones shown in Figure 4.4 are only for illustration purposes and do not affect the simulation experiment.

The primary objective of the experiment is to investigate the structure of the queue formed by the pairs of following agents. A key aspect of this structure is the inter-pair distance, which is illustrated in Figure 5.1 through a series of histograms. Specifically, each histogram captures the distribution of distances between a given pair and the pair immediately in front of it. The analysis of these histograms reveals that the distance between the first and second pair is comparable to the distances between the second and third pair and the third and fourth pair. The distances have a variance, which is natural

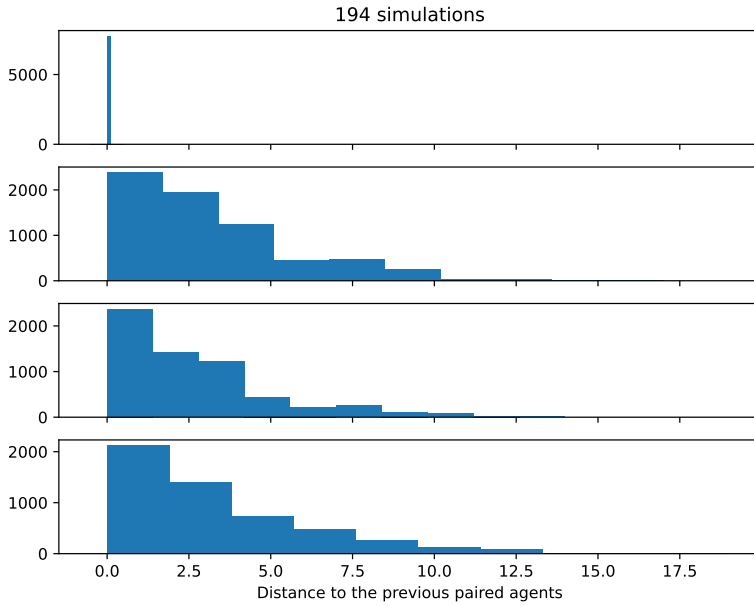


Figure 5.1: Distance between individual pairs in map `gaps.txt` and `gaps_back.txt` is consistent. Each histogram shows a distance of a pair to pair in front of them. The *y* axis shows counts of the distances in the investigated area across all simulations.

to the movement of people in a queue and qualitatively correspond to the movement of children in pairs.

The simulation parameters *Baseline* used in almost 200 runs can be seen in the Table 4.2.

5.2 Pair formation

One goal of the model was to capture the movement of pairs of children. Once two following agents form a pair, it is assumed they will stay together until they are close to the evacuation cell. Figure 5.2 depicts the distance of individual agents to the leading agent throughout the whole simulation. The distance of individual agent was calculated by collecting distance at every step in the simulation, averaged across all runs and then smoothed using rolling average with windows size 2.

Three scenarios on the same map with long corridor `map01.txt`, `map02.txt`, `map03.txt` were analyzed. As can be seen in the Figure 5.2, once the following agents are paired and pass the bottleneck (noisy part of the graphs at early stage of evacuation), the agents move together, keeping same distance to the leader as their partner agent - the paired agents plot similar line.

The first scenario features the goal of navigating to the exit. The second scenario's goals are to form a group in the classroom, move to the location B and only then navigate to the exit. In both scenarios, the leading agent position was at the front of the queue. These two scenarios show small difference in the dynamics as can be also seen in the specific flow graphs in Figure 5.8.

Also a group split is worth noting, as can be seen in the graph as few agents had low distance to the leading agent, while other agents were left behind and their distance increased until the congestion situation happened sometime around 200 model steps.

Opposite to this is the third scenario, where the leading agent was positioned at the

back of the group and managed to keep the group more compact as can be seen on the y axis, where highest distance is 22 compared to 35 in previous two scenarios. As expected, more distant agents evacuated the room earlier as the leader was positioned at the back, which is the opposite of the previous two scenarios.

The figures of three scenarios at map `map1X.txt` with shorter corridor are shown in Figure B.3 in the Appendix as they are comparable to the previous findings.

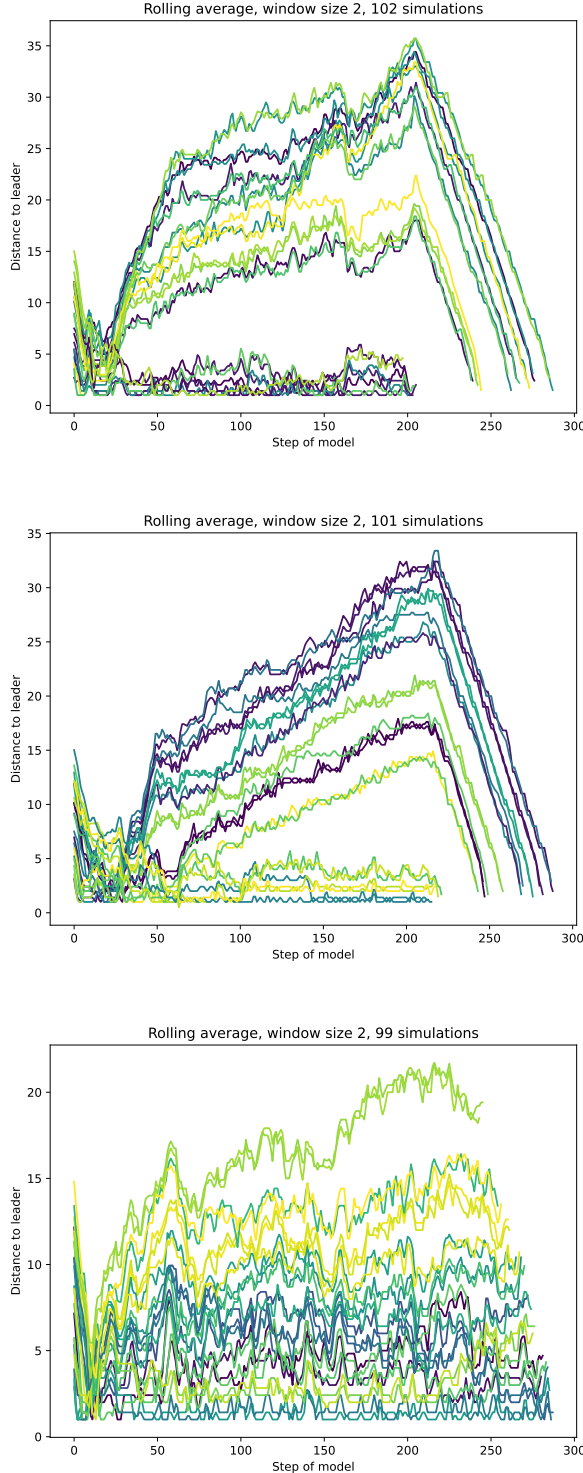


Figure 5.2: Distance of agents to the leader of `map01.txt` in the top figure, `map02.txt` in the middle figure, `map03.txt` in the bottom figure.

For completeness, three scenarios on the map with short corridor and right-turn `map21.txt`, `map22.txt`, `map23.txt` are depicted in Figure 5.3. The first scenario is comparable to the situation in `map01.txt` as the leading agent is navigating to the exit. The distance of paired agents increases in time up to the congestion situation. The second scenario follows the goals and rules described in the Table 5.1. The last rule makes the agent positioned at the back of the group as he navigates the group towards the exit. There is less difference in the distances of agents and the value does not evolve in time, which can be attributed to the agent position at the back. The last scenario included a rule of leading agent waiting at a location C. After evacuating the classroom and reaching location B, the agent departs from the group and waits for them at the corner apex. This is shown in the bottom graph as the sharp spike in distances of agents.

Another finding can be spotted in the Figure 5.4, where paired agents have same similar distances to the leader and its variance. The closer the pair is to the agent, the less variance is in the distance, which supports influence of *discipline* on following agents, described in Section 2.3.3.

5.3 Symmetry of the experiments

The structure of a pair of following agents consists of a leader, positioned on the right in the direction of the orientation. This can raise question whether such requirement might result in *asymmetric* movement or other form of *biased* movement. The following simulation experiments were run on mirrored versions of the maps described in Table 4.2. The map topology was mirrored on the x axis, as well as initial positions of the agents and the goals.

The two Figures 5.5 depict two heatmaps of visits of the cells, which are almost identical apart from the mirrored topology. The most complex map and scenario `map23.txt` was selected to allow all kinds of movements to be present.

Also, the boxplot graphs of the agents' distance to the leader in Figure 5.6 shows comparable variance and average values of distance of agents to the leading agent in the original and mirrored simulation experiments. This provides further evidence to support the claim, that the structure of agents' pair does not result in asymmetric movement or other form of biased movement.

In more than 100 simulations, further quantitative analysis revealed that the average TET was 178.29 ± 5.63 steps in map `map23.txt`, and 178.94 ± 4.84 in map `map23_mirror.txt`. Moreover, the TET in other maps was found to be comparable in both the original and mirrored versions.

5.4 Total evacuation time

TET is averaged across more than 100 simulations in three different maps `map0X.txt`, `map1X.txt`, `map2X.txt`. The first digit in map name indicates the topology and second digit in map name indicates scenario type as was explained in Table 4.2. Each map contains three scenarios with different goals such as navigating to a location, waiting for following agents to form a queue and different rules as position of the leading agent at the front or at the back of the queue and standing guard at a location. The TET values averaged over all simulations can be seen in Table 5.1.

In the *Baseline* simulation experiments a leading agent was present, and the following agents formed pairs. The *No Leader, No Pairs* simulation experiments did not have a leading agent and the following agents did not form pairs. The *Leader, No Pairs* simulation experiments had a leading agent present but the following agents did not form pairs. The

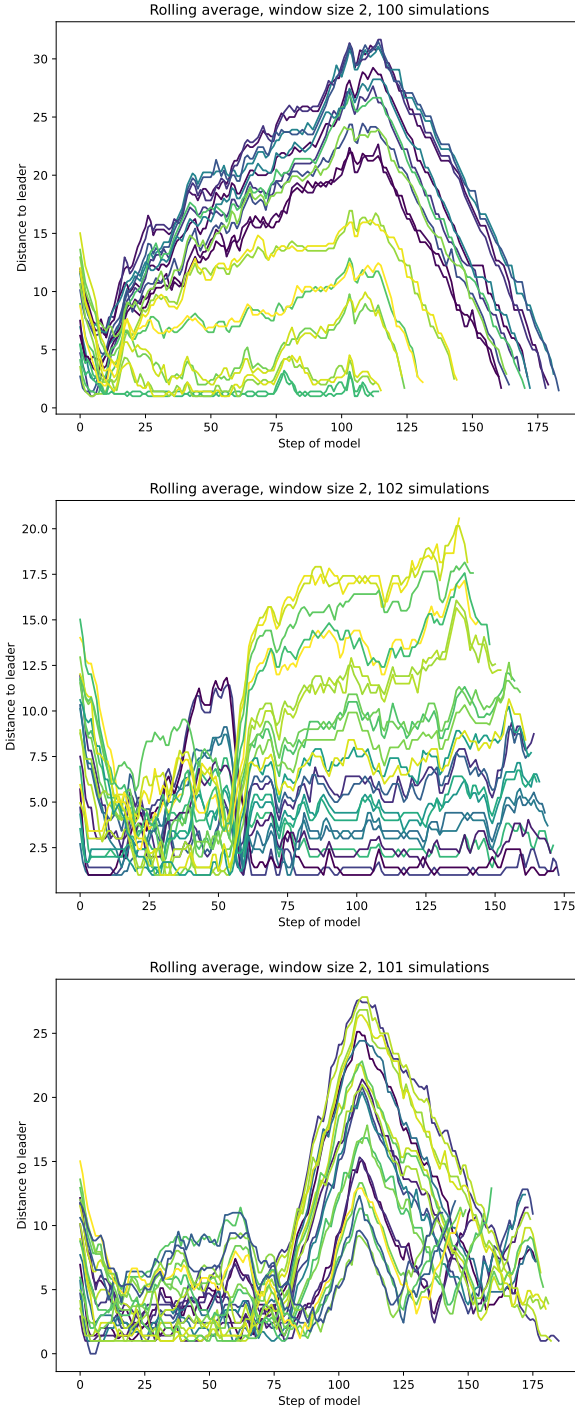


Figure 5.3: Distance of agents to the leader of `map21.txt` in the top figure, `map22.txt` in the middle figure, `map23.txt` in the bottom figure.

last simulation experiments *Optimal path* were done with a single leading agent moving optimally without any following agents present.

The highest TET is on map type `map0X.txt` which features long corridor. Simulation experiments with leading agent and following agents without forming pairs have lowest TET across all maps, which can be attributed to the following agents better ability to pass through the bottleneck of class door (width of 2 cells).

Simulation experiments *No Leader, No Pairs* have comparable TET to the *Baseline* even though this method is very unlikely to happen in real world. As Najmanová noted

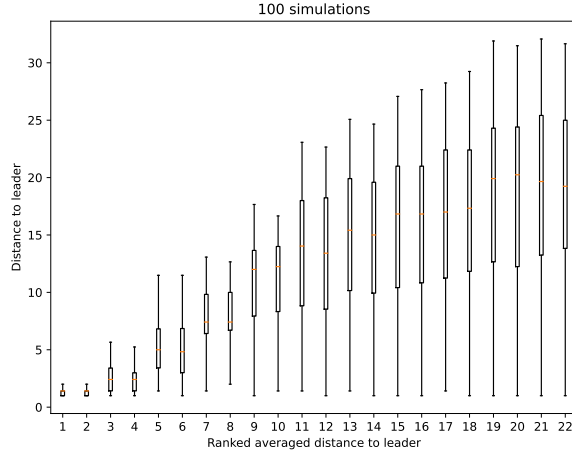


Figure 5.4: Distribution of distances of agents to the leading agent in `map21.txt`.

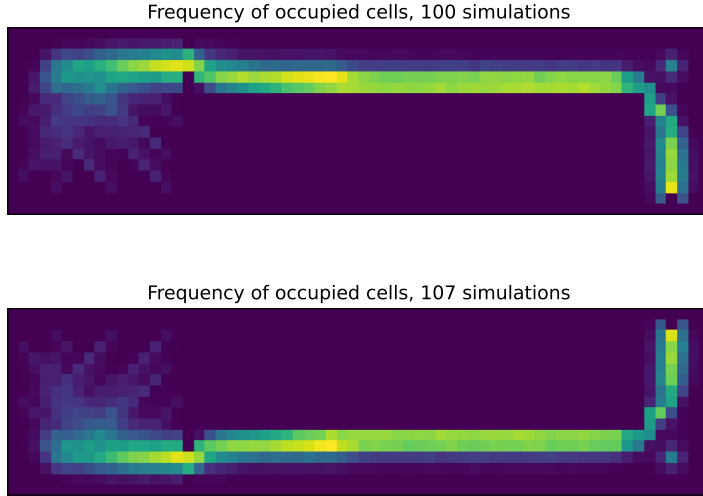


Figure 5.5: Heatmap of cell visits shows symmetry in `map23.txt` on top and the mirrored version below it.

in [7], children that are not assisted during evacuation do not necessarily select the most optimal exit, quite the opposite, and choose the familiar paths. Evacuation simulation experiments without leading agent are thus somewhat imaginary, because of the assumption that following agents know optimal evacuation path.

The *Baseline* simulation experiments show that adding goals to the evacuation leads to small increase in TET as can be seen in all maps across all scenarios. One exception is the scenario in map `map23.txt`, where leading agent stands guard at a location at the apex of the corner and evacuates as a last person. This scenario resulted in lower TET.

Across all maps and scenarios, TET in *Optimal path* set by single agent is close to half of TET in other simulations. This can be explained by the bottleneck situation at the single exit cell when $22 + 1$ agents reach the exit and evacuate one by one.

The exit choice, modeled as a single exit cell of 40 cm width could skew the simulation results because they model the preschool environment. Unlike adults, that evacuate one by one in doors of common width, children can evacuate through doors in pairs or alone[7]. Analyzing the influence of exit width is a space for further research.

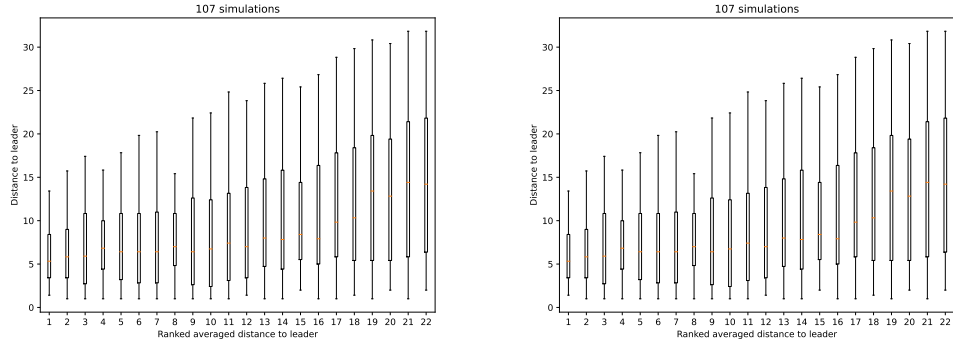


Figure 5.6: Boxplot of distances to the leading agent in original map `map23.txt` and mirrored map `map23.txt`.

Table 5.1: Comparison of path lengths for different scenarios

	Baseline	No Leader, No Pairs	Leader, No Pairs	Optimal path
<code>map01.txt</code>	277	279	257	146
<code>map02.txt</code>	281	278	269	148
<code>map03.txt</code>	287	279	277	148
<code>map11.txt</code>	160	170	152	76
<code>map12.txt</code>	166	170	164	84
<code>map13.txt</code>	173	170	171	84
<code>map21.txt</code>	175	183	166	83
<code>map22.txt</code>	186	183	183	92
<code>map23.txt</code>	178	183	176	98

5.5 Penalization parameter

The penalization parameter is used to discourage the selection of maneuvers that lead to incorrect orientation. As the value of this parameter increases, the frequency of such maneuvers decreases, as evidenced in Figures 5.7. The yellow dots represent the proportion of all maneuvers based on their distance to the leading agent, where a ratio of 0.15 at distance 1 indicates that 15% of all maneuvers occur at distance 1. The blue line, on the other hand, indicates the proportion of maneuvers resulting in incorrect orientation, specifically at the given distance. For instance, 0.3 at distance 1 implies that 30% of maneuvers at distance 1 resulted in incorrect orientation, which corresponds to ratio $0.15 \times 0.3 = 0.045$ of all maneuvers.

With penalization parameter set to 1, the ratio of incorrect maneuvers is almost not present at small distance to the leader (less than 10% of maneuver at said distance) and increases with distance where it does not cross 30% as can be seen in the Figure 5.7 in the last graph. The graphs do not show values in distances higher than 23, because too few maneuvers in this distance were spotted and the results would be skewed by stochasticity. With penalization parameter set to 0, the ratio of incorrect maneuvers is consistent across all distances to the leader, stabilised around 30% as is seen in the first graph. With penalization parameter of 0.5, the graph in the middle shows a decline in incorrect maneuvers for close distance but the rest of the blue line is comparable to the 0 penalization value. The yellow dotted plot of all maneuvers is comparable in all penalization parameter settings, which means that the ratio of maneuvers happening at various distances remained the same.

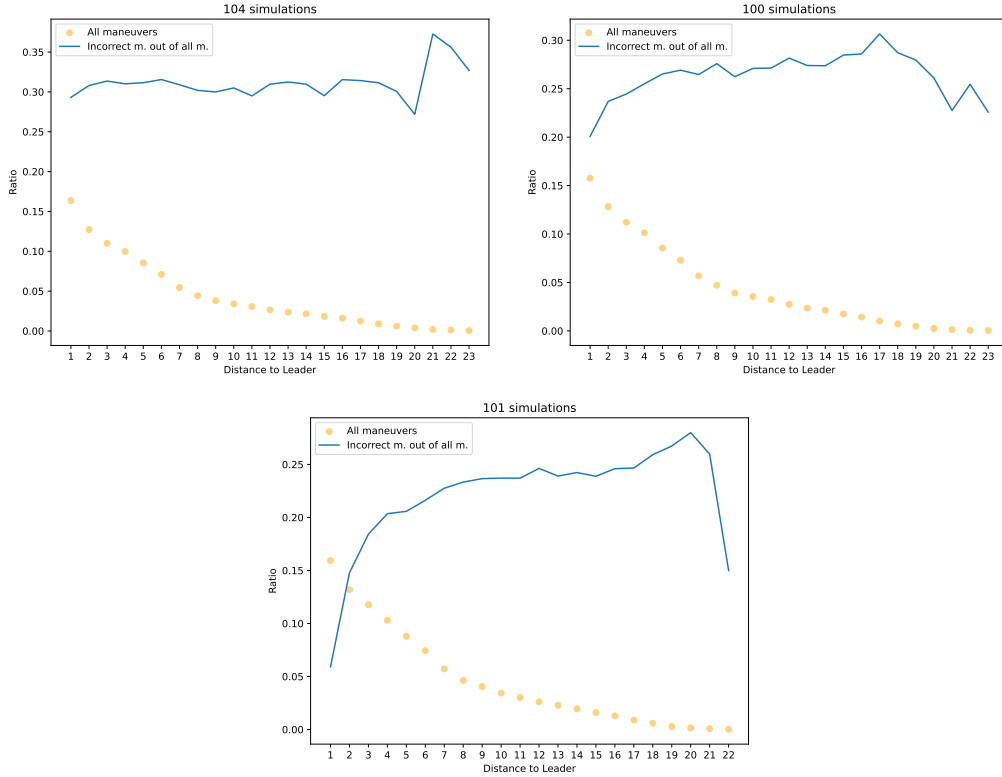


Figure 5.7: Penalization 0 in top figure, 0.5 in middle and 1 at the bottom. Ratio of maneuvers resulting in incorrect orientation decreases with higher penalization.

5.6 Specific flow

Specific flow of agents passing through three different gates explains the dynamics of the pedestrian movement. The first gate, called *Gate 0* is the classroom door of 2 cell width (0.8 m). Every agent needs to evacuate the classroom through this door. The specific flow in this gate can explain the pedestrian movement through bottleneck.

The second gate, called *Gate 1*, covers the whole width of the corridor with 5 cells (2 m) and is located on the x axis at position 51. This gate is situated after goal location B and aims to investigate the dynamics of agents moving in corridor. These two gates are present in all map types (`map0X.txt`, `map1X.txt`, `map2X.txt`).

The third gate, called *Gate 2* is present only in map with right-turn and covers the whole width of the corridor 5 cells (2 m) before the exit at y axis position 6. The y axis shows specific flow of persons passing certain line per time unit. Similarly to [11] and [7], the specific flow unit in these graphs is persons per meter per second ($\text{pers} \cdot s^{-1} \cdot m^{-1}$). Analysis of specific flow through this gate will explain how passing a turn affects the structure of the pedestrian crowd as well as congestion at the exit. The detailed definition of the gate positions can be found in the class `ExperimentSpecificFlow`.

The three Figures in 5.8 show specific flow in gate of the class door and in the middle of the corridor during three scenarios in the map `map0X.txt`.

The first scenario, with leading agent navigating directly to the exit has high flow in *Gate 0*. Because the agents do not form a group at location A, they leave the classroom sooner. Also, the smaller width of the door compresses the movement of agents and results in higher specific flow than in second scenario. The second scenario has slightly higher specific flow in *Gate 1*, which can be explained by the leader waiting for the group at location B and only when the group is compact again they move.

The third scenario has highest flow in *Gate 1*. The leading agent is positioned at the

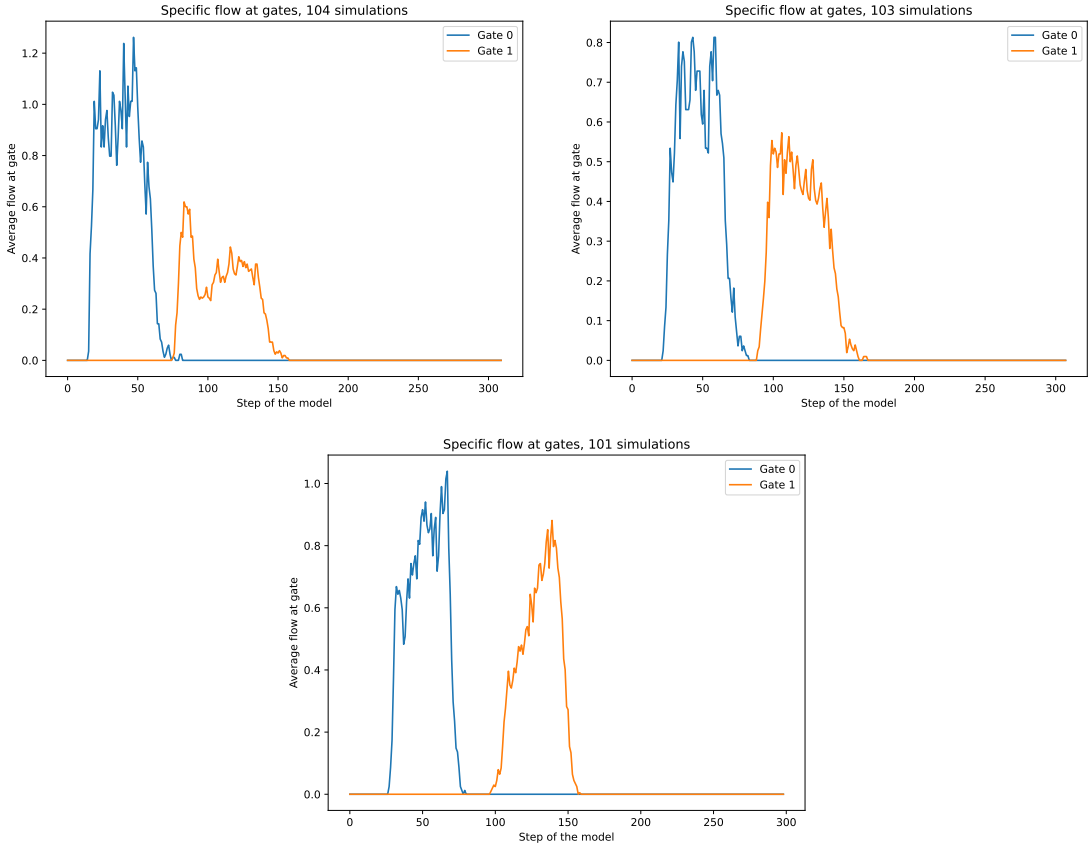


Figure 5.8: From left to right, top to bottom, specific flow for `map01.txt`, `map02.txt`, `map03.txt`.

back of the crowd and increases k_S of agents at the back. The agents then choose optimal movements more often and the flow is higher. Also, unlike in second scenario, the flow increases between steps 100 and 150, which means that majority of the agents is at the back near the leading agent. The first few agents create the low flow and with more and more agents approaching the gate, the flow increases. Opposite process happens in second scenario. Again, the leading agent waits for the agents at location B, which again makes the group more compact than first scenario.

The specific flow in bottleneck *Gate 0* ranges from 0.6 to $1.2 \text{ pers} \cdot s^{-1} \cdot m^{-1}$, which corresponds to the lower range in the findings of Najmanová, where the experimental research measured the specific flow of preschool children in the range from 0.65 to $4.17 \text{ pers} \cdot s^{-1} \cdot m^{-1}$ and mean value of 1.78 [7], other research measured the the mean value at $2.72 \text{ pers} \cdot s^{-1} \cdot m^{-1}$ [43].

The specific flow in wide corridor at *Gate 1* is much lower and ranges from 0.3 to $0.8 \text{ pers} \cdot s^{-1} \cdot m^{-1}$ in peaks. As can be seen in heatmap of visits in Figure 5.5, the agents move in the lower part of the corridor (width of three cells) and the remaining two cells are almost never visited. This results in the lower specific flow in all map results.

The specific flow of three scenarios in the map `map1X.txt` with shorter corridor is similar to previous map `map0X.txt`. The visualized specific flow is in the Figure B.2 in Appendix.

The three scenarios in the most complex map `map2X.txt` produced specific flows shown in the Figure 5.9. In all three scenarios, the figures show that dynamics of agent group movement did not change after passing the corner. The yellow line *Gate 1* shows the specific flow in the middle of the corridor before the corner and it is visually similar to the red line of *Gate 2* specific flow in the corridor after corner.

5. RESULTS

Notable deviation from the previous observation is the low specific flow in first scenario (leading agent navigating directly to the exit). In previous maps, this scenario produced highest flow, in this map the first scenario has the lowest flow in *Gate 0*. The highest specific flow can be found in the second scenario, where the agent is positioned at the back of the group after passing location B. The *Gate 1* area is located after location B, so it is affected by the leading agent's position at the back and the flow again increases in time, which can be explained by more agents being at the back of the crowd near the leading agent.

In the third scenario, the leading agent waits at location B and then moves to location C to stand guard there and navigate the following agents to the exit. The specific flow in the *Gate 1* and *2* is evenly spread.

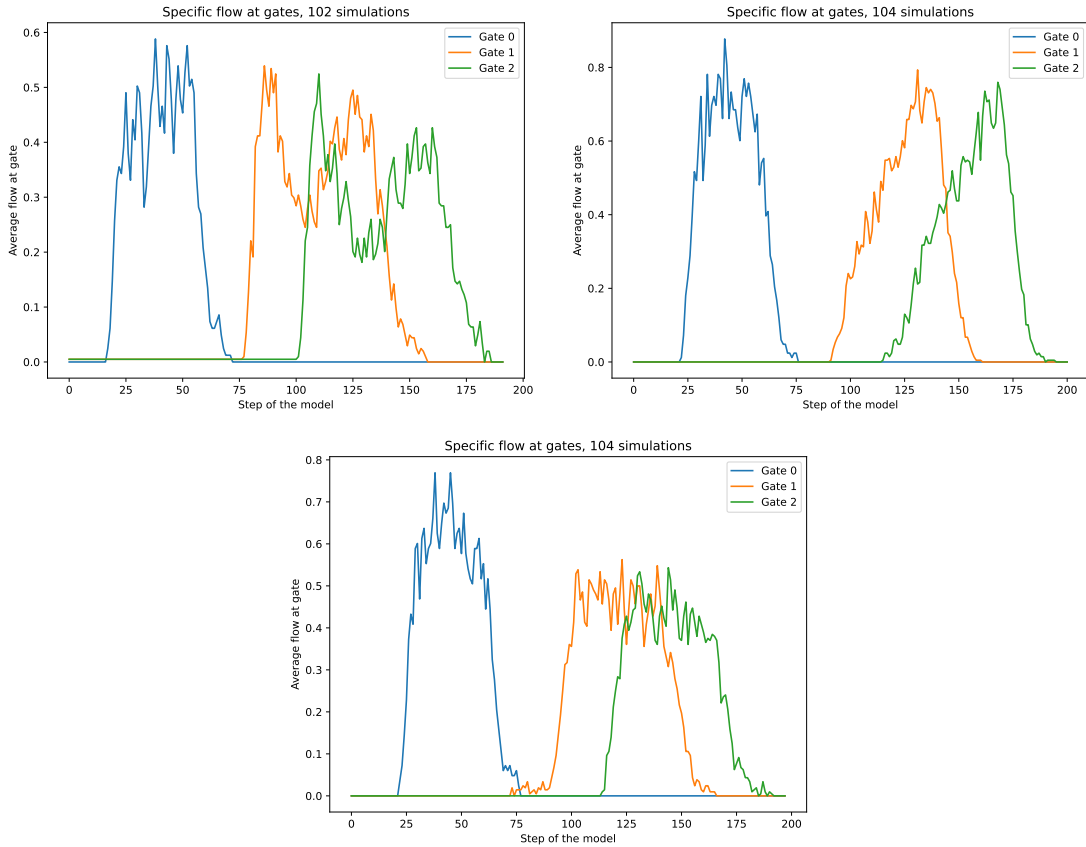


Figure 5.9: From left to right, top to bottom, specific flow for `map21.txt`, `map22.txt`, `map23.txt`.

5.7 Sensitivity to static field parameter

One of the parameters with major influence on the course and dynamics of the evacuation simulation is sensitivity to the static field k_S as was previously analysed in [31] where the study showed, that reasonable value range for this parameter lies somewhere in the range of $[1.5, 4.5]$.

The hierachical model in this study also depends on k_S and it is important to see how it affects the course of the simulation. As noted in the simulation parameters Table 4.2, there were three simulation experiments made with $k_S \in \{1, 3, 5\}$. The influence on the simulation is shown in Figure 5.10 using the heatmap of visits of cells. As k_S increased the heatmap trace became less dispersed.

With higher k_S , the agents choose the optimal cell more often and thus the movement is more deterministic. The graph on the top shows the simulation runs with low k_S , which produced erratic movement of agents across the whole width of the corridor and made the simulation much longer. Average TET was 250 ± 18.3 compared to 178.39 ± 5.68 in simulations with $k_S = 3$ and 171.43 ± 3.58 in simulations with $k_S = 5$.

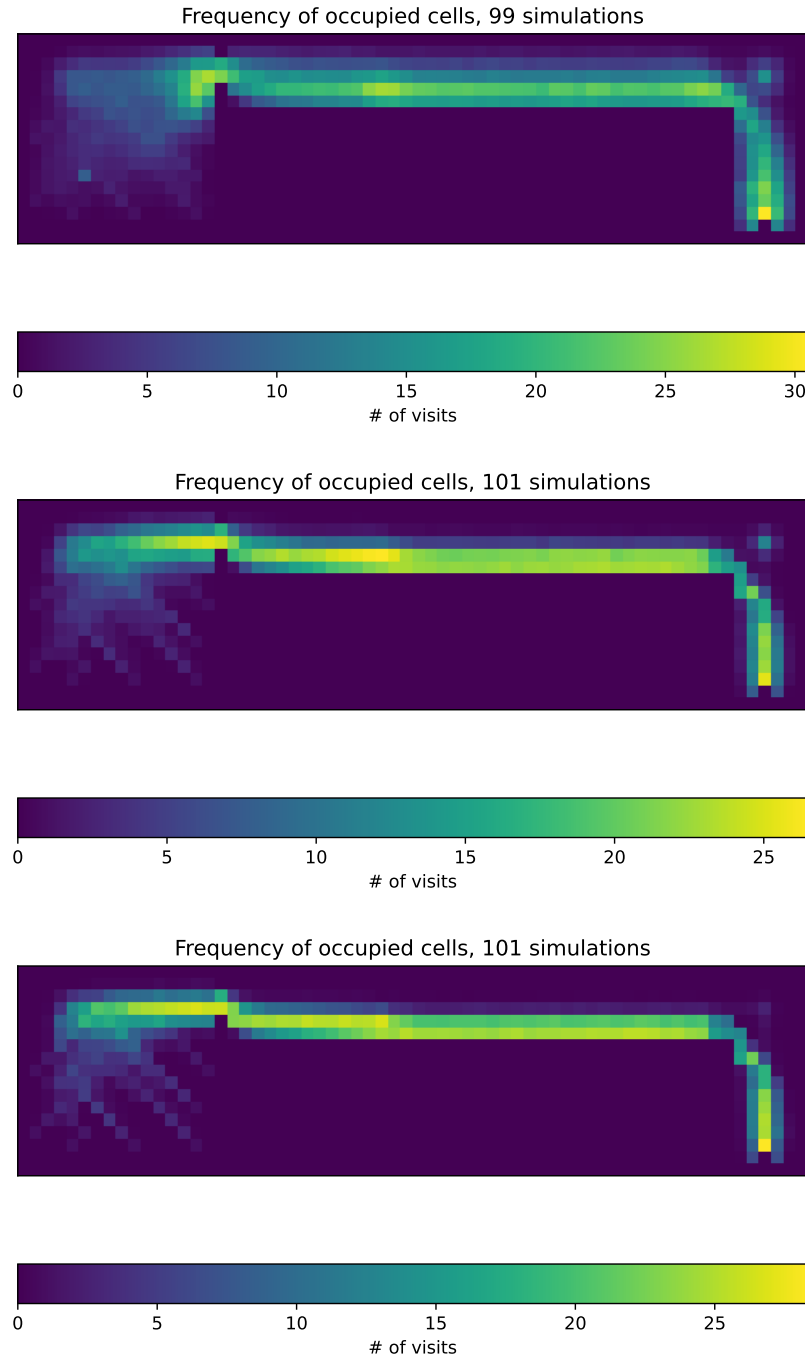


Figure 5.10: Heatmap of visits of cells in `map23.txt` with $k_S = 1$ in graph on the top, $k_S = 3$ in the middle, $k_S = 5$ on the bottom.

5.8 Sensitivity to occupied cell parameter

Higher k_O prevents the agent from choosing occupied cell for next move and prefers the side unoccupied cells. As can be seen in the Figure 5.11, where with increasing k_O the trace of agents made by visiting cells is more spread out and the agents do not follow the leader in packed queue but rather move in whole width of the corridor. Also, the maximal number of visits, as shows the colorbar, is higher for low k_O , which means the group of agents was more compact as they spread less and visited fewer unique cells.

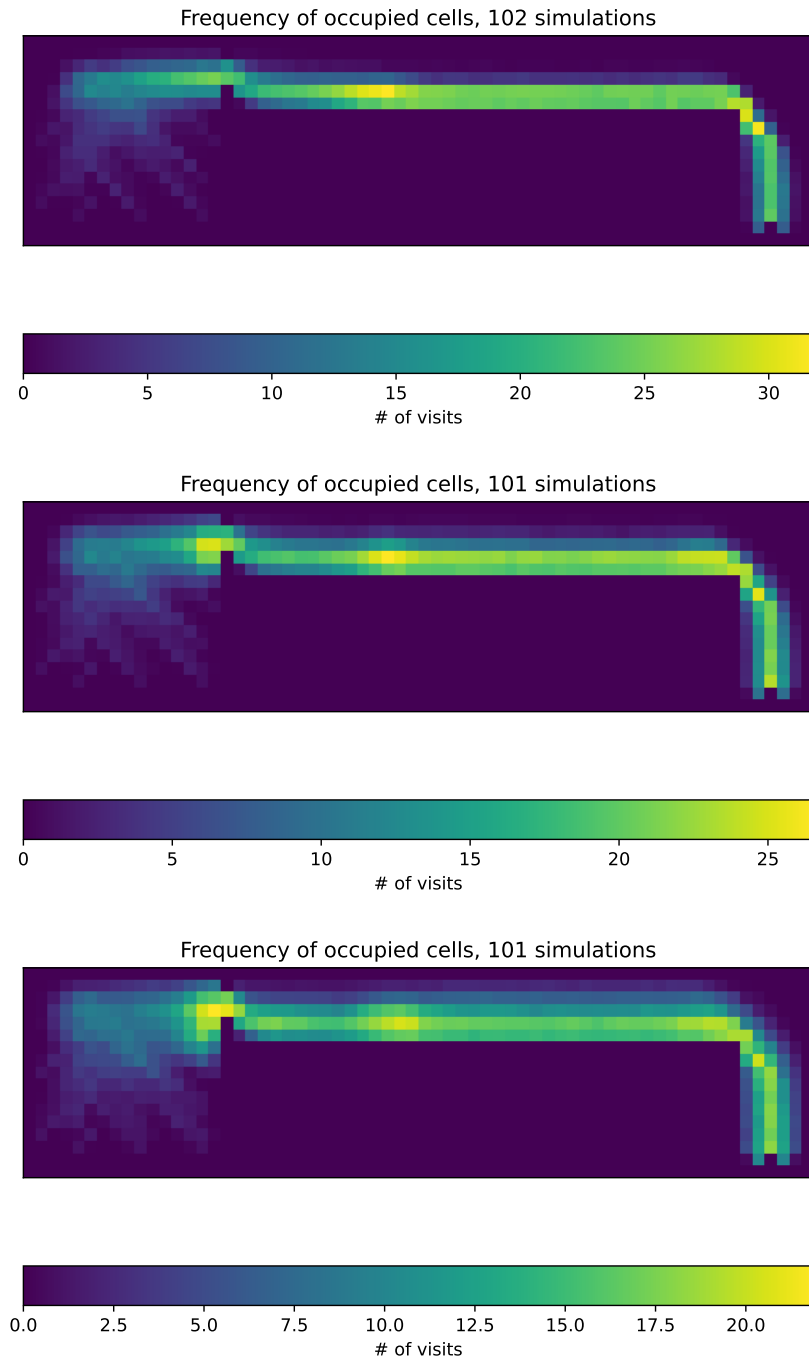


Figure 5.11: k_O with values of 0 on the top, 0.5 in the middle and 1 on the bottom in `map22.txt`.

The paired agents that move in queue need to select the cell in front of them to move

in tightly packed group. Once the probability of choosing it is zero because of the $k_O = 1$, the paired agents can choose to stay in their cell and create gaps between the pairs. The gaps are present even if $k_O > 0$ as was analysed in Section 5.1, so the high k_O parameter affects the course of the evacuation mostly in bottlenecks, when pairs are grouped together without gaps.

5.9 Limitations

Discussions with fire engineering experts were conducted to capture the qualitative aspects of children's behavior during guided evacuation, followed by several simulation experiments on different maps to analyze the quantitative aspects of the simulation. However, in order to validate and test the model's ability to simulate evacuation, further experimental simulations and comparisons with experimental evacuation results are necessary. Also, the model parameters were not calibrated to match simulation results with experimental results.

One disadvantage of the proposed hierarchical model is its discretized nature, which reduces the resolution of movement, a well-known drawback of CA models. Additionally, the proposed strategies and methods are rather inflexible (the leading agent can only be at the front or back of the crowd, pair formation consists of only two agents in adjacent non-diagonal cells, etc.) and may not fully express the latent behavior characteristics of people during evacuation.

While the proposed model is based on previous research of evacuation simulations and uses up-to-date approaches, incorporating it into a general simulation system would be challenging due to its lack of flexibility. Developing an agile, general, and customizable system that allows researchers to easily incorporate new methods and build upon previous work would be a significant challenge but promises great rewards

Conclusion

This study aimed to study the behavior characteristics of children during evacuation observed in experimental research, and proposed a hierarchical simulation model based on the expert consultation with fire engineering expert.

The proposed hierarchical model uses the structure of leading and following agents and offers a novel approach to simulate the evacuation of children, which captures the behavior and movement of children as observed in real life. The unique perspective on the evacuation of children is based on a predefined structure of paired agents and the strategies and rules of the leading agent.

The qualitative analysis of the simulation experiments provides insights into the effects of various parameters on the total evacuation time, specific flow, and crowd structure. The results show that the strategies and parameters proposed in this study significantly influence the evacuation process, and thus demonstrate the importance of considering the behavior and movement characteristics of children during evacuation.

Despite the success of the proposed model, there are limitations that need to be addressed in future research. One limitation is the discretized nature of the proposed hierarchical model, which may lower the resolution of movement. Additionally, the proposed strategies and methods are rigid and may not fully capture the latent behavior characteristics of people during evacuation.

However, the proposed model operates with up-to-date approaches and can be incorporated into general simulation systems with further development. Creating a flexible and customizable system that allows researchers to easily incorporate new methods and build on previous work is a significant challenge, but one that holds great promise for future research.

Overall, this study contributes to the field of evacuation modeling by providing a novel approach to simulating the evacuation of children that captures their behavior and movement characteristics. The proposed model and its associated methods and strategies provide valuable insights into the evacuation process, which can be used to improve evacuation planning and preparedness for vulnerable populations such as children.

Bibliography

- [1] Najmanová, H.; Kuklík, L.; et al. Evacuation trials from a double-deck electric train unit: Experimental data and sensitivity analysis. *Safety Science*, volume 146, 2022: p. 105523, ISSN 0925-7535, doi:<https://doi.org/10.1016/j.ssci.2021.105523>. Available from: <https://www.sciencedirect.com/science/article/pii/S0925753521003660>
- [2] Gorrini, A.; Bandini, S.; et al. Group Dynamics in Pedestrian Crowds Estimating Proxemic Behavior. *Transportation Research Record: Journal of the Transportation Research Board*, volume 2421, January 2014: pp. 47–55, doi:10.3141/2421-06.
- [3] CHEN, H.; WANG, X.; et al. Formation flight of fixed-wing UAV swarms: A group-based hierarchical approach. *Chinese Journal of Aeronautics*, volume 34, no. 2, 2021: pp. 504–515, ISSN 1000-9361, doi:<https://doi.org/10.1016/j.cja.2020.03.006>. Available from: <https://www.sciencedirect.com/science/article/pii/S1000936120301205>
- [4] Barnes, B.; Dunn, S.; et al. Improving human behaviour in macroscale city evacuation agent-based simulation. *International Journal of Disaster Risk Reduction*, volume 60, 2021: p. 102289, ISSN 2212-4209, doi:<https://doi.org/10.1016/j.ijdrr.2021.102289>. Available from: <https://www.sciencedirect.com/science/article/pii/S2212420921002557>
- [5] Chen, L.; Tang, T.-Q.; et al. Child behavior during evacuation under non-emergency situations: Experimental and simulation results. *Simulation Modelling Practice and Theory*, volume 90, 2019: pp. 31–44, ISSN 1569-190X, doi:<https://doi.org/10.1016/j.simpat.2018.10.007>. Available from: <https://www.sciencedirect.com/science/article/pii/S1569190X18301539>
- [6] Han, T.; Zhao, J.; et al. Smart-Guided Pedestrian Emergency Evacuation in Slender-Shape Infrastructure with Digital Twin Simulations. *Sustainability*, volume 12, no. 22, 2020, ISSN 2071-1050. Available from: <https://www.mdpi.com/2071-1050/12/22/9701>
- [7] Najmanová, H. *Evacuation of Pre-school Children Aged from 3 to 6 Years*. Dissertation thesis, Czech Technical University in Prague, 2021.
- [8] Yang, X.; Yang, X.; et al. Guide optimization in pedestrian emergency evacuation. *Applied Mathematics and Computation*, volume 365, 2020: p. 124711, ISSN 0096-3003, doi:<https://doi.org/10.1016/j.amc.2019.124711>. Available from: <https://www.sciencedirect.com/science/article/pii/S0096300319307039>

- [9] Gu, Z.; Liu, Z.; et al. Video-based analysis of school students' emergency evacuation behavior in earthquakes. *International Journal of Disaster Risk Reduction*, volume 18, 2016: pp. 1–11, ISSN 2212-4209, doi:<https://doi.org/10.1016/j.ijdrr.2016.05.008>. Available from: <https://www.sciencedirect.com/science/article/pii/S2212420916300371>
- [10] Kuligowski, E.; Gwynne, S. The Need for Behavioral Theory in Evacuation Modeling. Pedestrian Evacuation Dynamics 2008, Wuppertal, GE, 2010-02-01 2010. Available from: https://tsapps.nist.gov/publication/get_pdf.cfm?pub_id=861543
- [11] Predtechenskii, V.; Milinskii, A. *Planning for Foot Traffic Flow in Buildings*. TT, Amerind, 1978, ISBN 9780862493264. Available from: <https://books.google.cz/books?id=3AZaPwAACAAJ>
- [12] Chen, L.; Tang, T.-Q.; et al. Empirical investigation of child evacuation under non-emergency and emergency situations. *Journal of Transportation Safety & Security*, volume 14, no. 4, 2022: pp. 585–606, doi:[10.1080/19439962.2020.1793858](https://doi.org/10.1080/19439962.2020.1793858), <https://doi.org/10.1080/19439962.2020.1793858>. Available from: <https://doi.org/10.1080/19439962.2020.1793858>
- [13] Larusdottir, A.; Dederichs, A. Evacuation of children - movement on stairs and on Horizontal Plane. *Fire Technology*, volume 48, no. 1, 2012: pp. 43–53, ISSN 0015-2684, doi:[10.1007/s10694-010-0177-6](https://doi.org/10.1007/s10694-010-0177-6).
- [14] Xie, W.; Lee, E. W. M.; et al. A study of group effects in pedestrian crowd evacuation: Experiments, modelling and simulation. *Safety Science*, volume 133, 2021: p. 105029, ISSN 0925-7535, doi:<https://doi.org/10.1016/j.ssci.2020.105029>. Available from: <https://www.sciencedirect.com/science/article/pii/S0925753520304264>
- [15] Haghani, M.; Sarvi, M.; et al. Dynamics of social groups' decision-making in evacuations. *Transportation Research Part C: Emerging Technologies*, volume 104, 2019: pp. 135–157, ISSN 0968-090X, doi:<https://doi.org/10.1016/j.trc.2019.04.029>. Available from: <https://www.sciencedirect.com/science/article/pii/S0968090X18307009>
- [16] Chen, L.; Tang, T.-Q.; et al. Elementary students' evacuation route choice in a classroom: A questionnaire-based method. *Physica A: Statistical Mechanics and its Applications*, volume 492, 2018: pp. 1066–1074, ISSN 0378-4371, doi:<https://doi.org/10.1016/j.physa.2017.11.036>. Available from: <https://www.sciencedirect.com/science/article/pii/S0378437117311123>
- [17] Ruan, X.; Zhou, J.; et al. An improved cellular automaton with axis information for microscopic traffic simulation. *Transportation Research Part C: Emerging Technologies*, volume 78, 2017: p. 63 – 77, doi:[10.1016/j.trc.2017.02.023](https://doi.org/10.1016/j.trc.2017.02.023), cited by: 55. Available from: <https://www.scopus.com/inward/record.uri?eid=2-s2.0-85014742122&doi=10.1016%2fj.trc.2017.02.023&partnerID=40&md5=fcb31577557b5639dc033273226b4487>
- [18] Kougioumtzoglou, G.; Theodoropoulos, A.; et al. A Guide for the Development of Game-Based Evacuation Simulators. In *Educating Engineers for Future Industrial Revolutions*, edited by M. E. Auer; T. Rüütmann, Cham: Springer International Publishing, 2021, pp. 554–566.
- [19] Games, M. The fantastic combinations of John Conway's new solitaire game "life" by Martin Gardner. *Scientific American*, volume 223, 1970: pp. 120–123.

- [20] Rendell, P. Turing Universality of the Game of Life. 01 2001: pp. 513–539, doi: 10.1007/978-1-4471-0129-1_18.
- [21] Li, Y.; Lu, C.; et al. Simulation of a pediatric hospital in evacuation considering groups. *Simulation Modelling Practice and Theory*, volume 107, 2021: p. 102150, ISSN 1569-190X, doi:<https://doi.org/10.1016/j.smpat.2020.102150>. Available from: <https://www.sciencedirect.com/science/article/pii/S1569190X20300897>
- [22] Hassanpour, S.; Rassafi, A. A.; et al. A hierarchical agent-based approach to simulate a dynamic decision-making process of evacuees using reinforcement learning. *Journal of Choice Modelling*, volume 39, 2021: p. 100288, ISSN 1755-5345, doi:<https://doi.org/10.1016/j.jocm.2021.100288>. Available from: <https://www.sciencedirect.com/science/article/pii/S175553452100021X>
- [23] Izquierdo, J.; Montalvo, I.; et al. Forecasting pedestrian evacuation times by using swarm intelligence. *Physica A: Statistical Mechanics and its Applications*, volume 388, no. 7, 2009: pp. 1213–1220, ISSN 0378-4371, doi:<https://doi.org/10.1016/j.physa.2008.12.008>. Available from: <https://www.sciencedirect.com/science/article/pii/S0378437108009953>
- [24] Hrabák, P.; Bukáček, M. Influence of agents heterogeneity in cellular model of evacuation. *Journal of computational science*, volume 21, 2017: pp. 486–493.
- [25] Janovská, K. *Hierarchické řízení rojů při evakuaci*. B.S. thesis, Czech Technical University in Prague, 2022.
- [26] Hoogendoorn, S.; Daamen, W. Self-organization in pedestrian flow. In *Traffic and Granular Flow'03*, Springer, 2005, pp. 373–382.
- [27] Lian, L.; Mai, X.; et al. An experimental study on four-directional intersecting pedestrian flows. *Journal of Statistical Mechanics: Theory and Experiment*, volume 2015, no. 8, aug 2015: p. P08024, doi:10.1088/1742-5468/2015/08/P08024. Available from: <https://dx.doi.org/10.1088/1742-5468/2015/08/P08024>
- [28] Rodriguez, S.; Amato, N. M. Behavior-based evacuation planning. In *2010 IEEE International Conference on Robotics and Automation*, 2010, pp. 350–355, doi: 10.1109/ROBOT.2010.5509502.
- [29] Yang, Y.; Yu, J.; et al. Multiagent Collaboration for Emergency Evacuation Using Reinforcement Learning for Transportation Systems. *IEEE Journal on Miniaturization for Air and Space Systems*, volume 3, no. 4, 2022: pp. 232–241, doi: 10.1109/JMASS.2022.3210531.
- [30] Selvek., R.; Surynek., P. Engineering Smart Behavior in Evacuation Planning using Local Cooperative Path Finding Algorithms and Agent-based Simulations. In *Proceedings of the 11th International Joint Conference on Knowledge Discovery, Knowledge Engineering and Knowledge Management - KEOD*, INSTICC, SciTePress, 2019, ISBN 978-989-758-382-7, ISSN 2184-3228, pp. 137–143, doi: 10.5220/0008071501370143.
- [31] Šutý, M. *Conflict solution in cellular evacuation model*. B.S. thesis, Czech Technical University in Prague, 2021. Available from: <https://dspace.cvut.cz/bitstream/handle/10467/95146/F8-BP-2021-Suty-Matej-thesis.pdf>
- [32] Nishinari, K.; Kirchner, A.; et al. Extended Floor Field CA Model for Evacuation Dynamics. *IEICE Transactions on Information and Systems*, volume E87-D, 07 2003.

- [33] Huang, R.; Zhao, X.; et al. Static floor field construction and fine discrete cellular automaton model: Algorithms, simulations and insights. *Physica A: Statistical Mechanics and its Applications*, volume 606, 2022: p. 128150, ISSN 0378-4371, doi:<https://doi.org/10.1016/j.physa.2022.128150>. Available from: <https://www.sciencedirect.com/science/article/pii/S0378437122007099>
- [34] Hrabák, P.; Bukáček, M. Conflict solution according to “aggressiveness” of agents in floor-field-based model. In *Parallel Processing and Applied Mathematics: 11th International Conference, PPAM 2015, Krakow, Poland, September 6-9, 2015. Revised Selected Papers, Part II*, Springer, 2016, pp. 507–516.
- [35] Hrabák, P.; Bukáček, M.; et al. Cellular Model of Room Evacuation Based on Occupancy and Movement Prediction: Comparison with Experimental Study. *J. Cell. Autom.*, volume 8, no. 5-6, 2013: pp. 383–393.
- [36] Bukáček, M.; Hrabák, P.; et al. Cellular model of pedestrian dynamics with adaptive time span. In *Parallel Processing and Applied Mathematics: 10th International Conference, PPAM 2013, Warsaw, Poland, September 8-11, 2013, Revised Selected Papers, Part II 10*, Springer, 2014, pp. 669–678.
- [37] Kazil, J.; Masad, D.; et al. Utilizing Python for Agent-Based Modeling: The Mesa Framework. In *Social, Cultural, and Behavioral Modeling*, edited by R. Thomson; H. Bisgin; C. Dancy; A. Hyder; M. Hussain, Cham: Springer International Publishing, 2020, pp. 308–317.
- [38] Yap, W.; Janssen, P.; et al. Free and open source urbanism: Software for urban planning practice. *Computers, Environment and Urban Systems*, volume 96, 2022: p. 101825.
- [39] Leon-Blanco, J. M.; Gonzalez-R, P. L.; et al. A multi-agent approach to the truck multi-drone routing problem. *Expert Systems with Applications*, volume 195, 2022: p. 116604.
- [40] Ghanem, N.; Leitner, S.; et al. Balancing consumer and business value of recommender systems: A simulation-based analysis. *Electronic Commerce Research and Applications*, volume 55, 2022: p. 101195.
- [41] Vyhláška Ministerstva MMR č. 268/2009 Sb. Online, 2009, accessed: April 21, 2023. Available from: <https://mmr.cz/getmedia/2bf72909-e837-4dc8-9488-599950e8f9f6/Vyhlaska-MMR-268-2009>
- [42] Czech Statistical Office. České školy v číslech. <https://www.czso.cz/csu/stoletistatistiky/ceske-skoly-v-cislech>, 2019, accessed: April 21, 2023.
- [43] Kholshchevnikov, V. V.; Samoshin, D. A.; et al. Study of children evacuation from pre-school education institutions. *Fire and Materials*, volume 36, no. 5-6, 2012: pp. 349–366, doi:<https://doi.org/10.1002/fam.2152>, <https://onlinelibrary.wiley.com/doi/pdf/10.1002/fam.2152>. Available from: <https://onlinelibrary.wiley.com/doi/abs/10.1002/fam.2152>

APPENDIX A

Acronyms

ABM Agent-based model

CA Cellular automaton

SFF Static floor field

OFF Occupancy floor field

TET Total evacuation time

Further graphical output

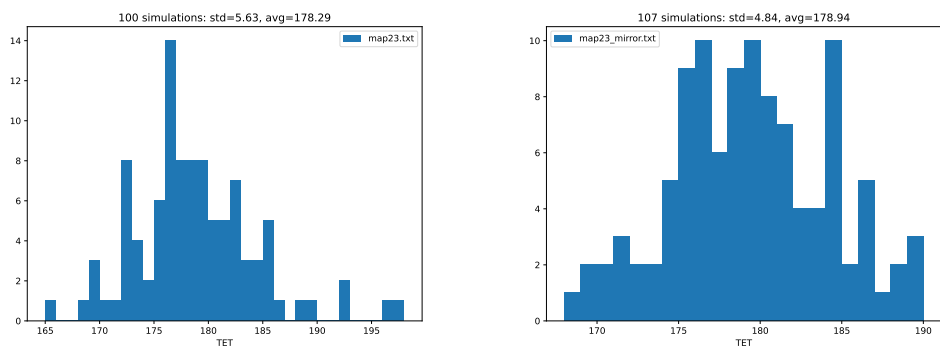


Figure B.1: Simulations with *Baseline* parameters in `map23.txt` on the left and in `map23_mirror.txt` on the right show comparable distribution of TET.

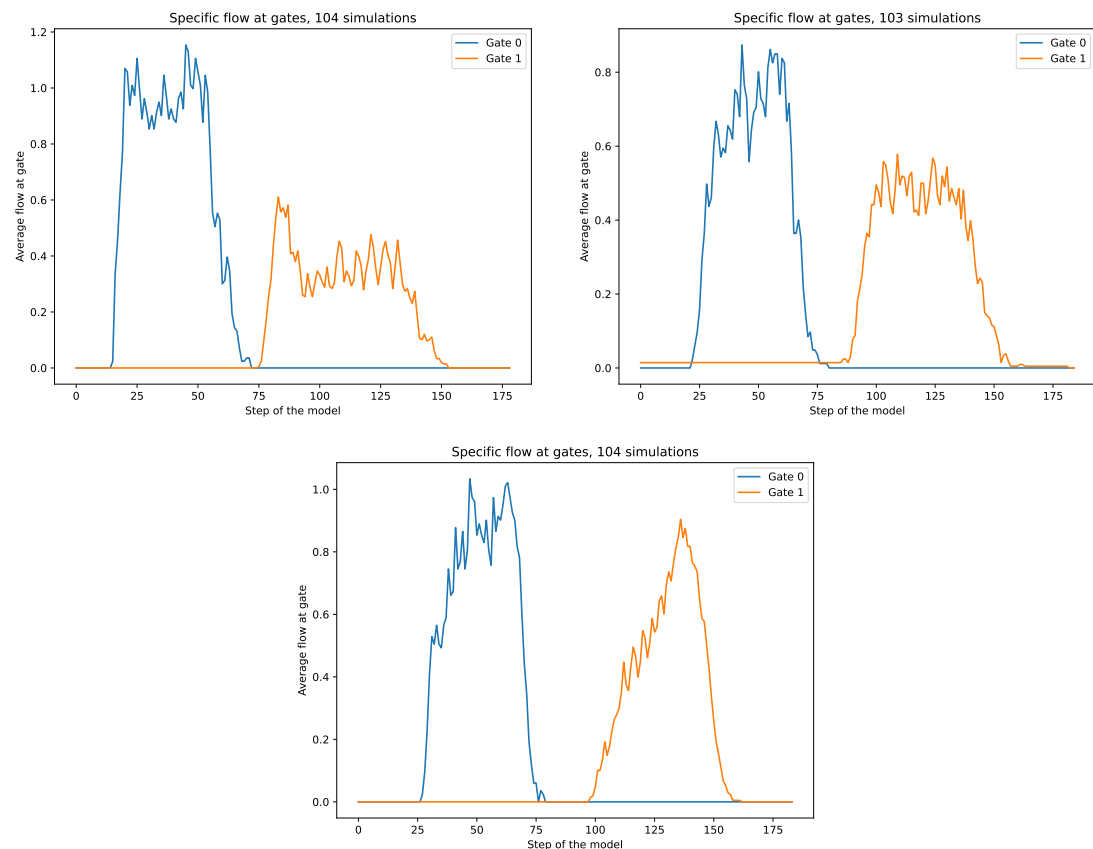


Figure B.2: From the left top to right bottom, specific flow for `map11.txt`, `map12.txt`, `map13.txt`.

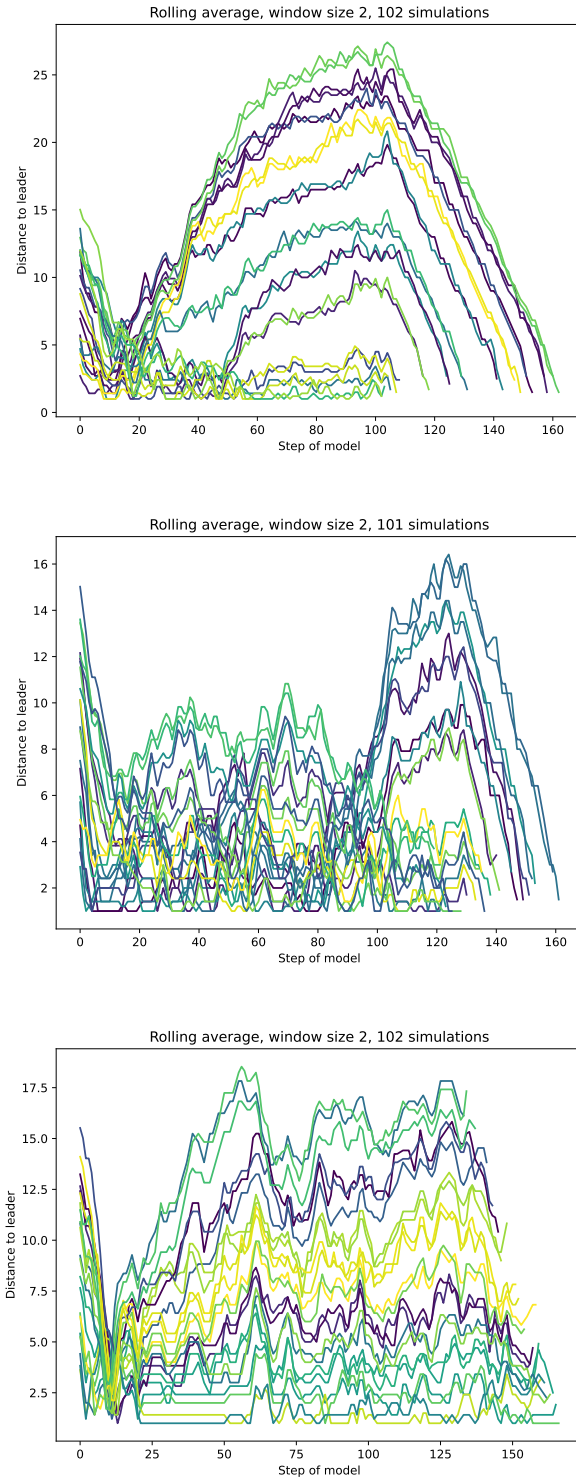


Figure B.3: Distance of agents to the leader of `map11.txt` in the top figure, `map12.txt` in the middle figure, `map13.txt` in the bottom figure.

Contents of enclosed CD

readme.txt	the file with CD contents description
code	the directory of source codes
roommodel	implementation sources
thesis	the directory of L ^A T _E X source codes of the thesis
thesis.pdf	the thesis text in PDF format